Available online at www.sciencedirect.com
ScienceDirect
Micron 39 (2008) 495–516
micron
www.elsevier.com/locate/micron

Review

Cyclodextrin-based aggregates and characterization by microscopy

Yifeng He, Pei Fu, Xinghai Shen *, Hongcheng Gao

Beijing National Laboratory for Molecular Sciences (BNLMS), Department of Applied Chemistry, College of Chemistry and Molecular Engineering, Peking University, Beijing 100871, China

Received 30 March 2007; accepted 4 June 2007

Abstract

Cyclodextrin-based aggregates have been widely investigated with microscopies such as STM, AFM, SEM, TEM, and fluorescent microscopy to obtain the direct morphology and structure of samples. In the present review, we discuss various types of cyclodextrin aggregates, that is, native and modified cyclodextrins, inclusion complexes and their aggregates of cyclodextrins, cyclodextrin rotaxanes and polyrotaxanes, cyclodextrin nanotubes and their secondary assembly, and other high-order aggregates of cyclodextrins. Especially, we focus on the use of microscopy to characterize above aggregates. The application of modern microscopy tools promotes the investigation on cyclodextrins.

Keywords: Microscopy; Cyclodextrin; Aggregate; Assembly; Inclusion complex; Rotaxane; Nanotube

Contents

1. Introduction

Supramolecular chemistry, which is often defined as ''chemistry beyond the molecule'', is based on the molecular recognition (host–guest chemistry) to a great extent. The construction of supramolecular systems involves selective

* Corresponding author. Tel.: +86 10 62765915; fax: +86 10 62759191.
E-mail address: xshen@pku.edu.cn (X. Shen).

0968-4328/$ – see front matter © 2007 Elsevier Ltd. All rights reserved.
doi:10.1016/j.micron.2007.06.017

molecular combination between host and guest (Ariga and Kunitake, 2006). Among all potential hosts, the cyclodextrins seem to be the most important ones (Szejtli, 1998).

Cyclodextrins (CDs), which are produced from amylose fraction of starch by glucosyltransferases, are a series of cyclic oligomers consisting of six or more α-l,4-linked D-glucopyranose units (Saenger et al., 1998). Of all the CDs, the most abundant are α-, β-, and γ-CDs with six, seven and eight glucopyranoses, respectively. They have a rigid conical molecular structure with a hydrophobic interior and a hydrophilic exterior. The internal cavity can include a wide range of guest molecules, ranging from polar compounds such as alcohols, acids, amines, and small inorganic anions to apolar compounds such as aliphatic and aromatic hydrocarbons, while the hydrophilic exterior helps CDs to be solved in water (Hapiot et al., 2006). The driving force of the formation of inclusion complex comes from non-covalent interactions such as van der Waals forces, electronic effects, hydrophobic interactions, and steric factors (Rekharsky and Inoue, 1998). For CDs have been widely used in the chemical, pharmaceutical or food industry, and in the catalysis of mimic enzymes, the investigation on CDs is of remarkable significance.

Cyclodextrin aggregates investigated range widely from the aggregate of native CDs to high-order and complex ones. Here, we divide the cyclodextrin aggregates into five types: aggregates of native and modified CDs, inclusion complexes and their aggregates of CDs, cyclodextrin rotaxanes and polyrotaxanes, cyclodextrin nanotubes and their secondary assembly, and other high-order aggregates such as nanosphere and network aggregates. In this review, we will present a description about the above cyclodextrin aggregates and then focus on their characterization with available modern microscopies such as STM, AFM, SEM, TEM and fluorescent microscopy.

Recent progress in high-resolution STM imaging has allowed the visualization of the arrangements, orientations, and even inner structures of molecules in air, in ultrahigh vacuum (UHV), and in solution (Ohira et al., 2003). Using this technology, self-organization of highly ordered molecular adlayers and/or two-dimensional (2D) supramolecular aggregations were investigated.

STM is a convenient and widely applied tool for the detection of the microstructures of supramolecular aggregates. Using STM, Li et al. have characterized an nanotube aggregates of diphenylhexatriene (DPH) with β-CD on highly orientated pyrolytic graphite (HOPG) (Li and McGown, 1994). However, it is rather difficult to interpret STM images of organic samples. In contrast, AFM is a relatively novel technique with which three-dimensional (3D) images can be obtained on the surface of insulating and conducting materials from nanometer to micrometer scale. Thus, AFM imaging of organic specimens is easier to perform as it does not require the specimen to be electron- or ion-conductive (Botella et al., 1996). AFM allows imaging under hydrated conditions without pre-treatment of the samples, however, the tip geometry and probe force usually lead to over-estimated lateral sizes of organic sample features and non-contact mode imaging has a maximum resolution of around 2 nm (Botella et al., 1996). AFM has been used successfully to image inclusion complexes and nanotubes, which will be discussed in detail in the following sections.

TEM and SEM imaging has no source–sample contacts and allows much higher resolution, however, it is usually carried out in high vacuum and requires pre-treatment of samples. The difference between TEM and SEM is that the surface topology can be obtained from SEM while more inner structure is given by TEM.

Fluorescent microscopy in the near-infrared between 950 and 1600 nm has been developed as a novel method of imaging and studying singlewalled carbon nanotubes (SWNTs) in a variety of environments. Also, it offers an important tool for the observation and characterization of cyclodextrin nanotubes (Wu et al., 2006c).

The above tools have been widely applied in obtaining the detailed information of structure, especially in the case that the single crystal for X-ray diffraction is difficult to prepare.

2. Aggregates of native and modified cyclodextrins

2.1. Aggregates of native cyclodextrins

2.1.1. The structure in crystal

There are two types of crystal structures for native CDs (α-, β-, and γ-CDs) as well as their inclusion complexes: cages and channels (Saenger et al., 1998). In cage-type complexes, the cavity of one cyclodextrin molecule is blocked off on both sides by adjacent CDs, thus making the guest molecules not contact with each other by isolated cavities. The cage-type structures have two different categories, i.e., herringbone and brick-type. In the former fashion, CDs are arranged crosswise (Fig. 1a); in the latter, CDs are stacked in layers like bricks in a wall (Fig. 1b). In crystal structures belonging to the channel type, cyclodextrin molecules are packed linearly on top of each other with "infinite" channels including guest molecules (Fig. 1c). The channels are straight only when a crystallographic symmetry axis coincides with the channel axis (Saenger et al., 1998). It is difficult to answer the question what are the conditions for formation of channel- or cage-type crystal structures except for α-CD with some extent of certainty. Typically, when α-, β-, and γ-CDs are crystallized as hydrate, the molecules are packed crosswise in herringbone fashion.

2.1.2. The structure in aqueous solution

Although CDs have been found for more than 100 years, the investigation on the self-aggregation of CDs in water is still rather limited by standard techniques of analysis (Azaroual-Bellanger and Perly, 1994; Bonini et al., 2006; Coleman and Nicolis, 1992; Gaitano and Brown, 1997; Gonzalez-Gaitano et al., 2002; Loftsson et al., 2004; Polarz et al., 2001; Szente et al., 1998). In general, native CDs can form aggregates in water with the size of about 200–300 nm, which depends on the CDs considerably (Bonini et al., 2006; Coleman and Nicolis, 1992; Gaitano and Brown, 1997; Gonzalez-Gaitano et al., 2002; Loftsson et al., 2004; Polarz et al., 2001; Wu et al., 2006b). For both α- and γ-CDs in aqueous solutions (25 g L^{-1}), Coleman

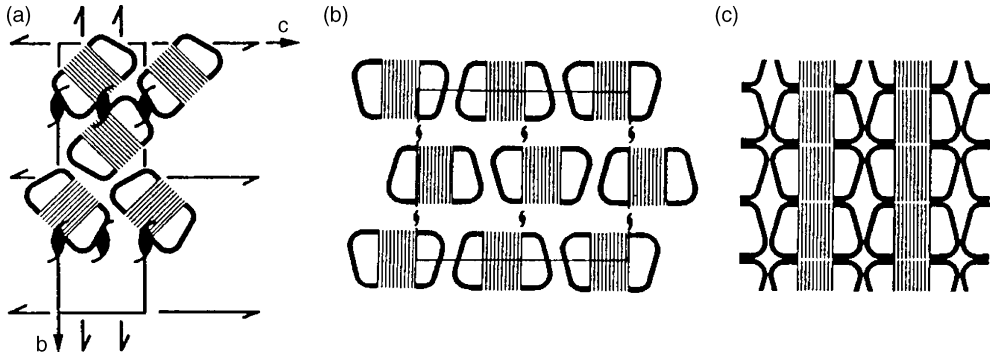

Fig. 1. Schematic description of (a) herringbone, (b) brick-type, and (c) channel crystal structures formed by cyclodextrin inclusion complexes. Reprinted from (Saenger et al., 1998).

and Nicolis (1992) found that the size of aggregates are about 200 nm. Gonzalez-Gaitano et al. reported that the aggregates could not pass through the 0.1 μm filter and that the filtrates were stable with time and no aggregates were formed again (Gaitano and Brown, 1997; Gonzalez-Gaitano et al., 2002). In the aqueous solution of β-CD, Coleman and Nicolis (1992) found that the aggregates with an average diameter of about 200 nm were dissociated and the solubility was sharply increased at the pH value higher than 12.5. They proposed a rod-like structure for the aggregates consisting of two chains of hydrated β-CD molecules. The above results suggested that the abnormally low solubility of β-CD in water could be ascribed to the presence of aggregates and their interaction with the surrounding water structure. However, using ^{2}H NMR, Azaroual-Bellanger and Perly (1994) detected only the β-CD monomer even in the closely saturated solution and on the time-scale of NMR. On the other hand, Gonzalez-Gaitano et al. (2002) discovered the formation of aggregates in the aqueous of β-CD, accompanied by non-associated monomers. The aggregates formed again with a fast aggregation kinetics even after filtering through 0.1 or 0.02 μm. The addition of urea or very high pH values induced the dissolution of the aggregates.

Using CDs assemblies as templates to produce mesoporous silica, Polarz et al. (2001) found wormlike structure and thus suggested that the cyclodextrin aggregate was expressed through a bicontinuous ''worm-type'' pore system with a diameter of about 1.5 nm (Fig. 2, left). Combining a semiempirical CNDO method, they believed that the cyclodextrin complexes preferred to line up in ideally parallel or staggered parallel arrangement with quadrupolar character (Fig. 2, right). Becheri et al. investigated the formation process of polypseudorotaxanes based on CDs and polymer like polyethylene-glycol (PEG) or polypropylene-glycol (PPG) and suggested that a preassembled, wormlike aggregate made up of several aligned CDs existed in aqueous solution (Becheri et al., 2003). The existence of cyclodextrin aggregates in water has also been found by Loftsson et al. (2004). According to their investigation, the aggregates, having non-inclusion complexation or micellelike structures, were able to solubilize lipophilic drugs. Through Cryo-TEM and light scattering experiments, Bonini et al. (2006) confirmed that β-CD monomers surely aggregated into polymorphism in different shape (Fig. 3) in water at room temperature, depending on the concentration of β-CD: polydisperse nearly spherical objects with diameters of about 100 nm were present at lower concentrations, whereas micrometer planar aggregates were predominant at higher concentrations. They indicated that the critical aggregation concentration of β-CD self-aggregation in water was between 2 and 3 mM, with a minimum hydrodynamic radius of about 90 nm. These particles were in equilibrium with larger objects at higher solute concentrations. Cryo-TEM images showed that disks and sheets coexisted and that upon sonication the large bidimensional sheets turned into entangled long fibers and folded lamellae. Static light scattering experiments were performed to evaluate the fractal nature of the particles (Bonini et al., 2006).

From the DLS results of our work (Fig. 4a), two kinds of size distribution in the aqueous solutions of CDs existed: one with mean hydrodynamic radius less than 1 nm and the other larger than 60 nm. The small size corresponded to the monomeric cyclodextrin and the large one to the self-aggregated cyclodextrin (Wu et al., 2006b). Furthermore, it was found that the monomeric forms of α-, β-, and γ-CDs were predominated in their aqueous solutions and that an equilibrium between the monomeric and aggregated forms of cyclodextrin existed. It should be pointed out here that we observed bimodal distribution for α-, β-, and γ-CDs when the samples were treated with 0.2-μm filter, while Gonzalez-Gaitano et al. just observed aggregated forms of β- and γ-CD with 0.2-μm filter and the monomeric form was detected with 0.1-μm filter. For α-CD, however, both monomeric and aggregated forms were detected even with 0.2-μm filter (Wu et al., 2006b). The self-aggregation of β-CD has also been studied by TEM, and large spherical aggregates of β-CD with diameter of 20–130 nm were observed (Fig. 4b). Similar spherical aggregates were observed for γ-CD in our previous work (Fig. 4c and d) (Wu et al., 2006b,c).

The driving force for the self-assembly of cyclodextrin molecules can be ascribed to hydrogen bonding considerably (Gaitano and Brown, 1997; Gonzalez-Gaitano et al., 2002; Polarz et al., 2001; Saenger et al., 1998; Szente et al., 1998). Some technical possibilities can be employed to reduce or remove the aggregates: (a) chemical modification of the hydroxyl groups on cyclodextrin molecules, (b) application of hydrogen-bond-disrupting agents such as urea, (c) increasing the pH of solutions to above pH 12 for the ionization of the

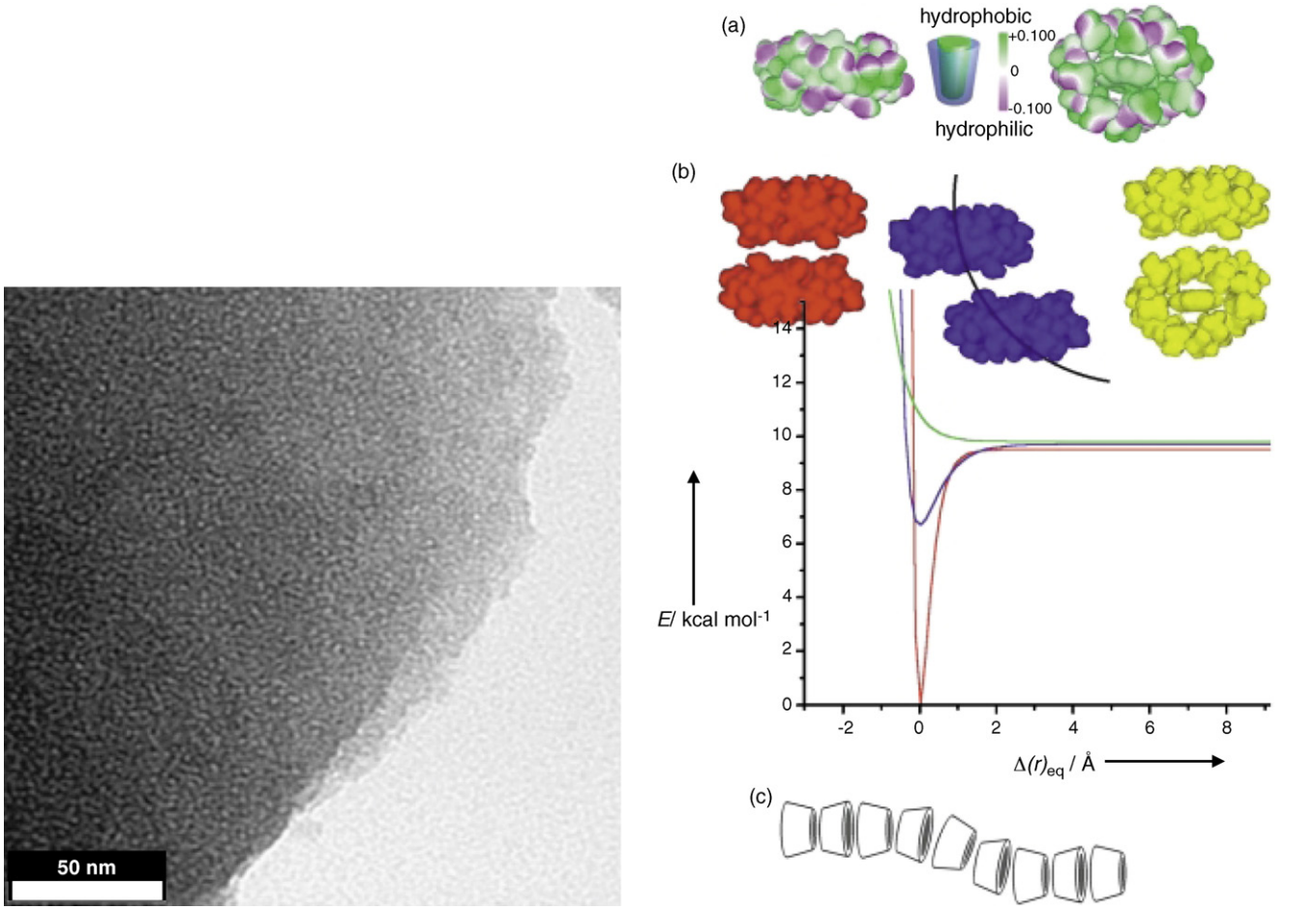

Fig. 2. Left: TEM image of α-CD-silica. Right: (a) MM2-calculated structure of a cyclodextrin inclusion complex and its electrostatic potential distribution from an ab initio Hartree–Fock calculation. (b) Calculated energy surfaces as a function of the inter-ring distance for the schematically shown ideally parallel (red), staggered (blue), and perpendicular (yellow) approach. (c) Schematic representation of the aggregate structure of α-CD, as revealed by silica nanocasting, dynamic light scattering, and SAXS in solution. Bright: hydrophilic domains; dark: hydrophobic domains. E = energy; $\Delta(r)_{eq}$ = deviance from equilibrium distance. Reprinted from Polarz et al. (2001).

hydroxyl groups of CDs, (d) high temperatures (Coleman and Nicolis, 1992; Gonzalez-Gaitano et al., 2002; Szente et al., 1998).

2.2. Aggregates of modified cyclodextrins

Cyclodextrins are chemically stable and can be modified in complete or regioselective manner leading to analogues with increased solubility and interesting complexing properties. They can undergo various reactions which may involve cleavage of OH, CO, CH or CC bonds. To simply substituted CDs such as 2,6-dimethyl-β-CD, the presence of the OH (3) hydroxyl groups may allow dimmerisation of the molecule (Coleman and Nicolis, 1992). The similar phenomena happens to hydroxypropylated (HP) α-, β-, and γ-CDs (1,6-hydroxypropyl groups per cyclodextrin) (Polarz et al., 2001). For the trimethyl derivative β-CD, however, no aggregation via hydrogen bonding is possible and only the monomeric structure has been detected (Coleman and Nicolis, 1992). Gonzalez-Gaitano et al. (2002) also found that partially substituted CDs such as methyl- and hydroxypropyl-β-CD (RAMEB and HP-β-CD, 12 mM) do not display significant aggregation. However, Olaf et al. reported on a strong enhancement in the viscosity of solutions of HP-β-CD with molecular substitution of 0.45 and 0.6, at concentrations beyond 50% and this phenomenon could be ascribed to the self-aggregation of HP-β-CD (Olaf and Muller-Goymann, 1993). McAlpine and Garcia-Garibay (1998) found that 3-*O*-(2-methylnaphthyl)-β-cyclodextrin formed dimmers at concentrations higher than 10^{-4} M, while in its dilute solutions only existed monomers.

Bügler et al. (1999) have synthesized two β-CD-calix[4]-arenes, one of which was found to form vesicles both with and without guest species, the other formed fibers, which changed into vesicles upon the addition of guest. The aggregates were visualized by TEM using both the freeze fracture technique and the uranyl staining method (see Fig. 5). Liu et al. (2003a) have compared the self-assembly behaviors of linear polymeric supramolecules formed by mono[6-*O*-(4-formyl-phenyl)-β-CD] in both solution and the solid state to reveal the general rule of the formation of dimmer (see Fig. 6). A hydrophobic cyclodextrin–porphyrin conjugate showed a marked tendency to dimerize in aqueous conditions via the formation of intermolecular porphyrin–cyclodextrin in inclusion complexes and/or through electrostatic interactions (Carofiglio et al.,

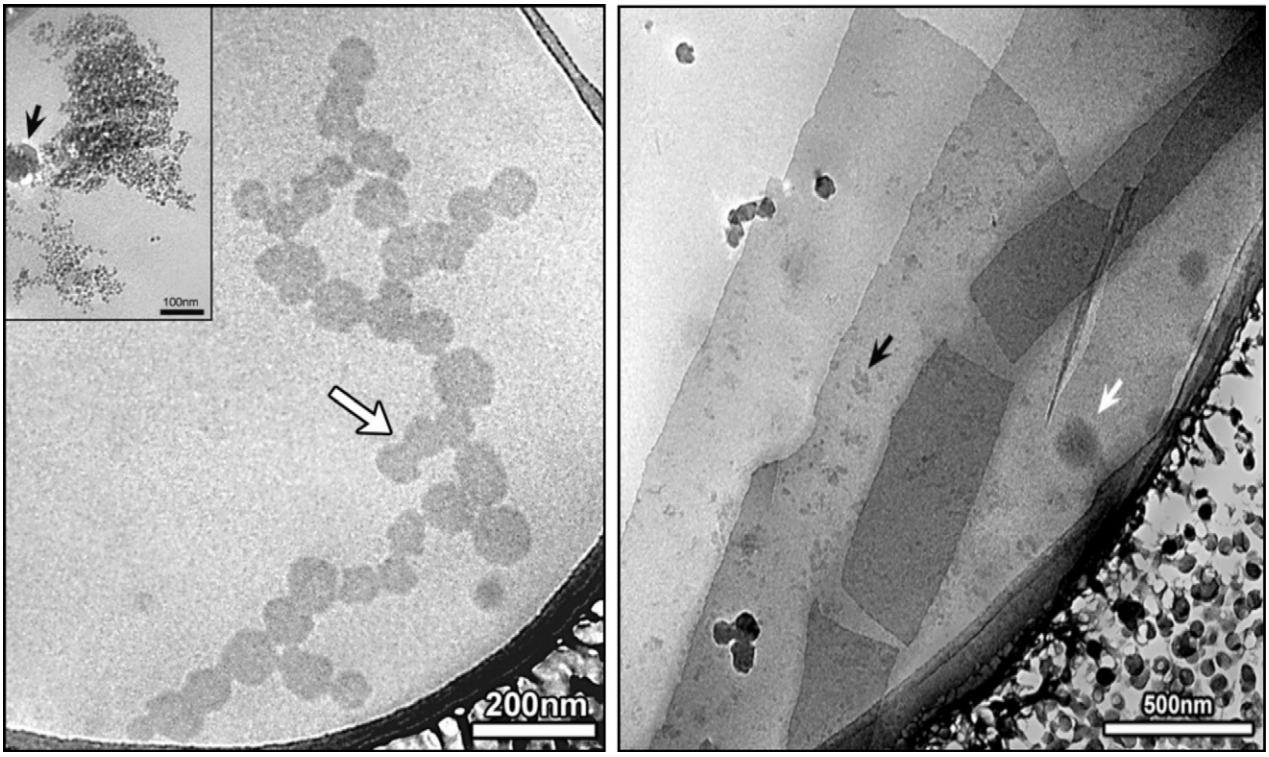

Fig. 3. Left: Cryo-TEM micrograph of a 3 mM β-CD/water solution vitrified from 25 °C, showing polyhedral aggregates in mutual contact to form a branched structure. (Inset) Globular particles shown from the same sample. The black arrow denotes an ice crystal deposited on the sample surface after vitrification. Right: Cryo-TEM micrograph of a 6 mM β-CD/water solution. The black arrow points at small globular particle attached to the sheet surface, whereas the white arrow indicates a discoidal aggregate. Reprinted from Bonini et al. (2006).

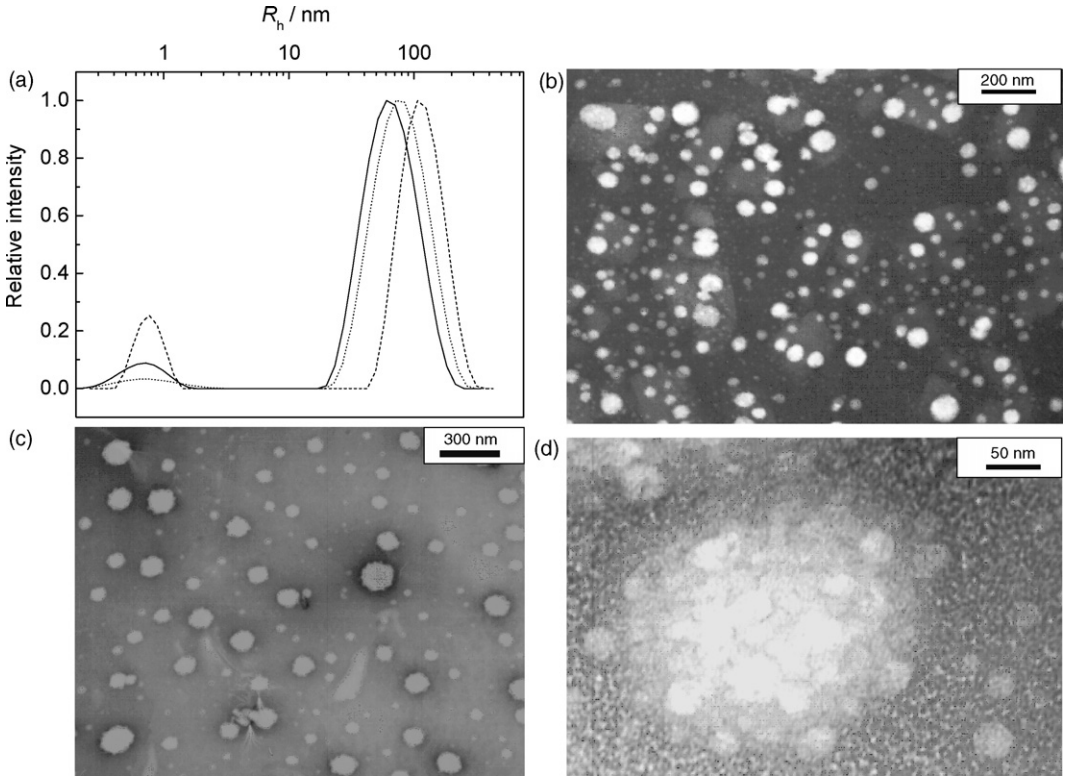

Fig. 4. (a) DLS results of the aqueous solutions of α-CD (solid line), β-CD (dash line), and γ-CD (dot line) treated with 0.2-μm filter; (b) TEM images of aggregated 10 mM β-CD; (c, d) TEM images of aggregated 10 mM γ-CD. Reprinted from Wu et al. (2006b,c).

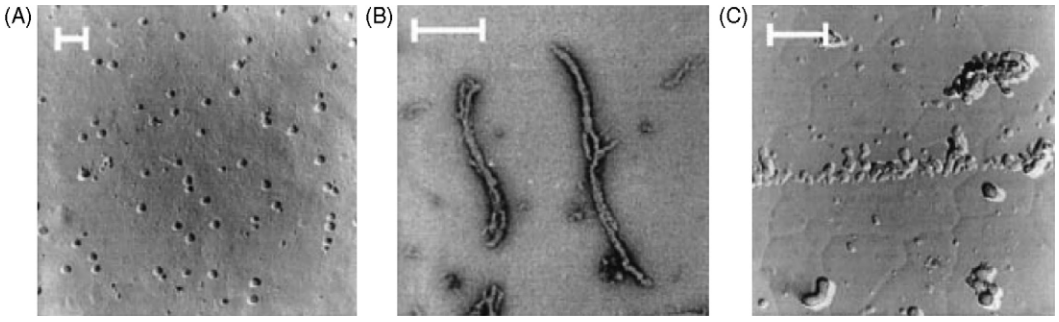

Fig. 5. Micrographs made by transmission electron microscopy. Each bar represents 200 nm. Concentrations were each 0.4 mg/mL in doubly distilled water. (A) β-CD-calix[4]arene **1** (freeze fracture), (B) β-CD-calix[4]arene **2** (uranyl staining), (C) β-CD-calix[4]arene **2** + 1 mmol/L 1-adamantanol (freeze fracture). Reprinted from Bügler et al. (1999).

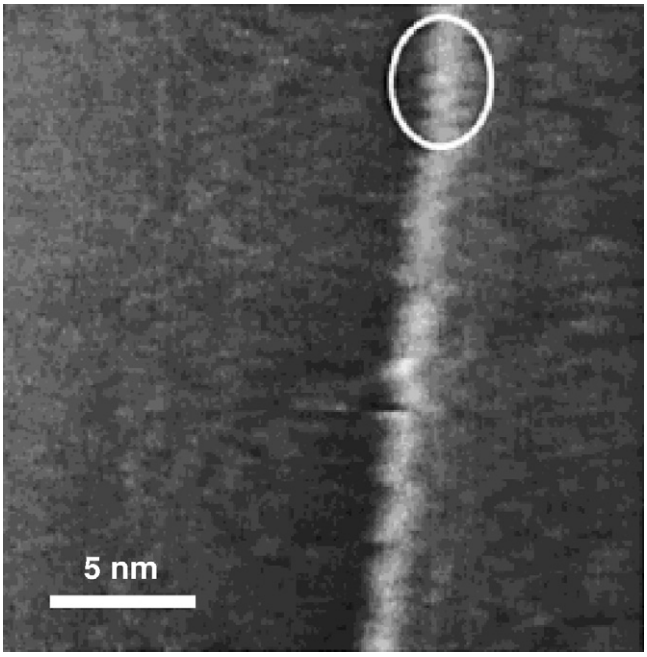

Fig. 6. STM image of supramolecular assembly of mono[6-*O*-(4-formyl-phenyl)-β-CD]. Reprinted from Liu et al. (2003a).

2000). A methylated cyclodextrin conjugating with a cholesterol derivative self-assembled into monodisperse spherical micelles with an average aggregation number of 24 (Auzely-Velty et al., 2000).

Modified amphiphilic CDs have been synthesized to design systems of drug molecules. The self-organization of various ionic and non-ionic amphiphilic CDs into stable monolayers and multilayers at the air-water interface and also in Langmuir–Blodgett films was investigated (Greenhall et al., 1995; Hamelin et al., 1999; Nakahara et al., 1996; Parazak et al., 1996; Tchoreloff et al., 1995). Thermotropic liquid crystals of CDs were also described (Ling et al., 1993). Darcy et al. reported on substituted cyclodextrin bilayer vesicles (Ravoo and Darcy, 2000). The heptakis[6-deoxy-6- alkylthio-2,3-oligo (ethylene glycol)]-β-CDs were synthesized in three step from β-CD. Through TEM, spherical vesicles with diameters of 50-300 nm were observed using uranyl acetate as a negative staining agent (Fig. 7, left). Later, they further investigated on the bilayer vesicles as host membranes that recognized guest molecules (Falvey et al., 2005). Also, they found that a β-CD substituted by amino and carboxymethyl groups on the primary and secondary side respectively, self-assembled in water into supramolecular tapes which were 50–300 nanometers wide and up to 20 μm long (Ravoo et al., 2001). Cyclodextrin vesicles could also be formed by amphiphilic β-CDs with alkylthio

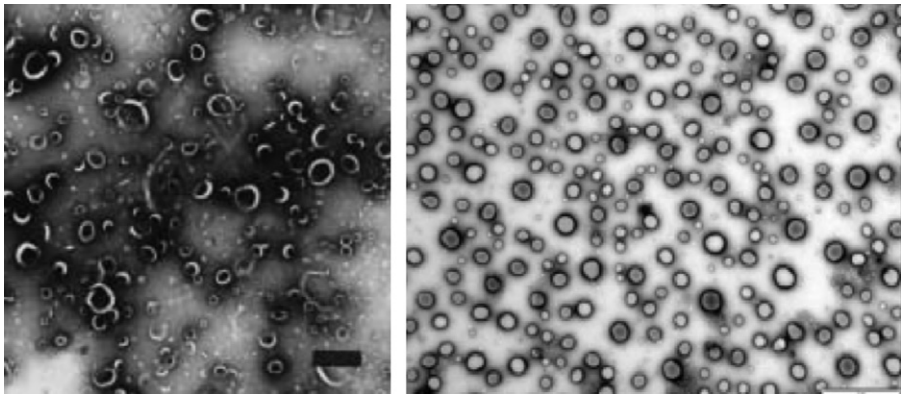

Fig. 7. Left: Electron micrographs of vesicles of sample. Vesicles obtained after 2 h sonication at 50 °C. The scale bars represent 500 nm. Reprinted from Ravoo and Darcy (2000). Right: Electron micrographs of ω-galactosyl β-CD in water (0.1 mg mL^{-1}). Negative staining with UO_2Ac. Scale bars = 2 μm. Reprinted from Mazzaglia et al. (2004).

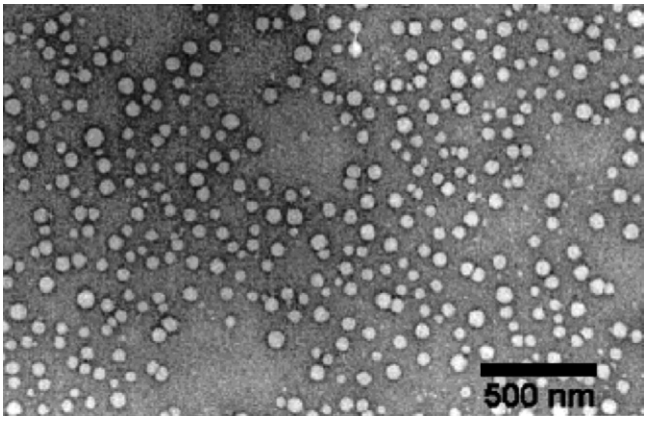

Fig. 8. Electron microscopy of nanoparticles of heptakis[6-deoxy-6-hexylthio-2-oligo (ethylene glycol)]-β-CD. Reprinted from Mazzaglia et al. (2002).

chains at the primary-hydroxyl side and galactosylthio-oligo-(ethylene glycol) units at the secondary-hydroxyl side (Mazzaglia et al., 2004) (Fig. 7, right).

Mazzaglia et al. synthesized three substituted CDs, i.e., heptakis[6-deoxy-6- alkylthio-2-oligo (ethylene glycol)]-β-CDs, one of which formed thermodynamically metastable nanoparticles with an average size of 50–150 nm (Fig. 8) and the other two formed stable micellar solutions in water (Lombardo et al., 2004; Mazzaglia et al., 2002). Wouessidjewe et al. have synthesized amphiphilic cyclodextrins which can self-aggregate into the nanoparticles (Choisnard et al., 2005, 2006; Gèze et al., 2002, 2004). Recently, they synthesized hexanoate and decanoate beta-cyclodextrin esters. Through cryo-TEM, the former appeared as uniformly dense nanospheres, whereas the latter exhibited a multilamellar onion-like organization (Choisnard et al., 2006). Kakuchi et al. have reported on the synthesis of end-functionalized polystyrenes (PSt) with β-CD, which was stably suspended in a good solvent for PSt by forming aggregates with β-CD as a core. The average aggregation numbers ranged from 42 to 125 (Kakuchi et al., 2003b). Also, they modified β-CD into a seven-functional initiator for 2,2,6,6-tetramethylpiperidinyloxy-(TEMPO-) mediated living radical polymerization, and obtained the seven-arm star PSt with a β-CD core which showed aggregation in a good solvent for PSt (Kakuchi et al., 2003a).

Mahalingam et al. have synthesized β-CD-functionalized silica nanoparticles with the relatively narrow particle size distribution (Fig. 9). Moreover, they showed the assembly of β-CD-functionalized silica nanoparticles on β-CD molecular printboards on silicon oxide through multivalent host–guest interactions employing the G5 adamantyl-terminated poly (propylene imine) dendrimer as a supramolecular glue (Fig. 10) (Mahalingam et al., 2004). Péroche et al. synthesized new amphiphilic CDs substituted at primary face by seven perfluorohexylpropanethiol, seven perfluorooctylpropanethiol chains or an average of four perfluorooctylpropanethiol chains. These molecules could self-assemble into nanospheres in aqueous media but alkylated analogue formed aggregates with sizes in the range from 60 to 350 nm (see Fig. 11) (Péroche et al., 2005). Six 2:1 cyclodextrin:[60]fullerene conjugates involving different types of linkers have been synthesized for search of a simple internal complexation of C60 in CDs. In water, these 2:1 cyclodextrin [60]fullerene monoadduct conjugates self-assembled into spherical micelles with no evidence to confirm the presence of a 2:1 inclusion complex, while in toluene they showed no sign of aggregation (Quaranta et al., 2006). SEM and AFM have been applied to the imagery of solid lipid nanoparticles formulated from an amphiphilic cyclodextrin, i.e., 2,3-di-*o*-alkanoyl-β-CD, β-CD21C6 (see Fig. 12) (Dubes et al., 2003).

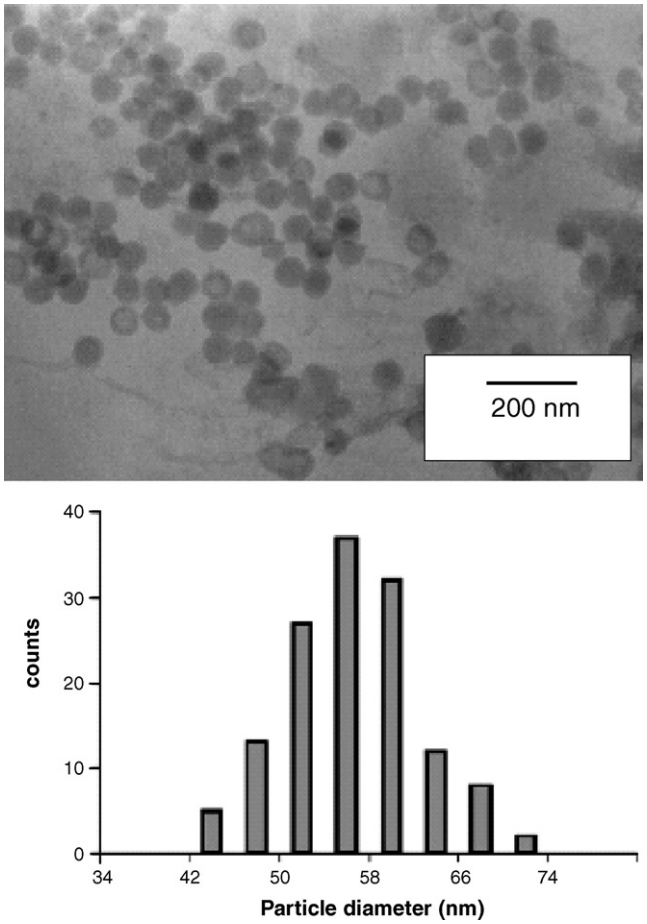

Fig. 9. TEM image (top) and histogram (bottom) showing the size distribution of β-CD-functionalized silica nanoparticles. Reprinted from Mahalingam et al. (2004).

3. Inclusion complexes and their aggregates of cyclodextrins

3.1. Inclusion complexes of cyclodextrins

The relatively hydrophobic cavity of CDs can accommodate various kinds of guest molecules to form inclusion complexes. The 1:1, 1:2 and 2:1 (guest:host) inclusion complexes are the most common types. Complexes in a stoichiometry of 2:2 (Avakyan et al., 1999; Clark et al., 2001; Dyck et al., 2003; Hamai, 1996; Hamai and Hatamiya, 1996; Nakamura et al., 1995; Sau et al., 2004; Wenz, 1994; Yang et al., 1997) can be

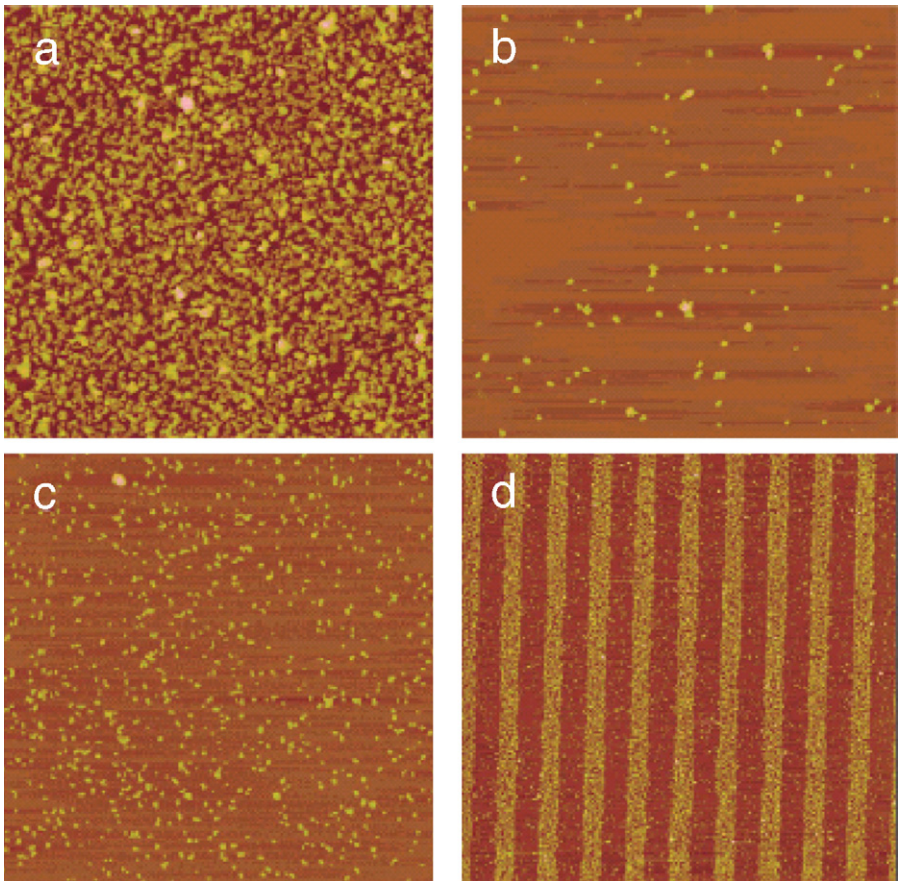

Fig. 10. AFM height images (z scale: a, b: 250 nm; c, d: 300 nm) obtained after the deposition (2 min at pH 9.2) of β-cyclodextrin- (a, b, d) and glucosamine-functionalized silica nanoparticles (c) on β-cyclodextrin printboards on silicon substrates with (a, c) and without (b) the preceding deposition of G5 adamantyl-terminated poly(propylene imine) dendrimers from solution or (d) the microcontact printing of the G5 dendrimers in 2-μm wide lines; image sizes are 10 μm × 10 μm and 50 μm × 50 μm for (a–c) and (d), respectively. Reprinted from Mahalingam et al. (2004).

also formed. Interestingly, ternary complexes of 1:1:1, 1:1:2, and 1:2:2 (guest A:guest B:host) have been reported (Du et al., 1996; Hamai, 1990, 1991, 2000; Kano et al., 1982; Selva et al., 1998; Shen et al., 1997). However, the 1:3 inclusion complexes are rarely reported. So far, the solid 1:3 inclusion complex between cholesterol and β-CD has been synthesized (Claudy et al., 1991). Several substituted 3H-indoles, i.e., iodotrimethyl 2-(*p*-hexylaminophenyl)- 3,3-dimethyl-5-carboethoxy-3H-indole ammonium, and iodo-methyldioctadecyl 2-(*p*- hexylaminophenyl)-3,3-dimethyl-5-carboethoxy-3H-indole ammonium formed 1:3 inclusion complexes with β-CD (Shen et al., 1998, 1999). Three homologues of iodo-methyl dihexadecyl 2-(*p*-oligoethyloxyethylene amino phenyl)-3,3-dimethyl-5-ethoxycarbonyl-3H-indole ammonium were synthesized and two of which were found to form the 1:3 rotaxane-like inclusion complexes with β-CD (Chen et al., 2005). Very recently, Mytides et al. (2006) reported on a 1:3 inclusion complex consisting of hydroxypropyl-β-CD and 2,2′:6′,2″-terpyridine. In addition, bovine serum albumin were found to form 1:3 or 1:4 inclusion complexes with some substituted mono- and bis-β-CDs (Gao et al., 2006). Functional-terminated dendrimer could form the well-defined 1:4, 1:8, 1:16, and 1:32 inclusion complexes with β-CD (Castro et al., 1997; Michels et al., 2000).

3.2. Aggregates of the inclusion complexes of cyclodextrins

Inclusion complexes of CDs are able to form larger aggregates in aqueous solutions, which can solubilize themselves or lipophilic water-insoluble drugs through non-inclusion complexation or micelle-like structures (Loftsson et al., 2004). Randomly methylated and hydroxypropyl β-CDs show formation of higher-order complexes or complex aggregates with triclosan and triclocarban form (Duan et al., 2005). Light scattering and NMR experiments provide evidence for the formation of large aggregates, like micelles, from β-carotene complexes with β- and γ-CDs in water (Mele et al., 1998). As shown in Fig. 13, the aggregates of inclusion complex were also found by AFM (Botella et al., 1996). In solid state, inclusion complexes of CDs may exhibit three types of crystal (see Section 2.1). To our knowledge, there is no general rule to judge which type of crystal an inclusion complex will be.

4. Cyclodextrin rotaxanes and polyrotaxanes

Rotaxane is a kind of molecular species consisting of linear components (so-called axis) threaded into cyclic components (so-called rings), where the dissociation of the ring from the axis is hindered by bulky groups (so-called stoppers) at both

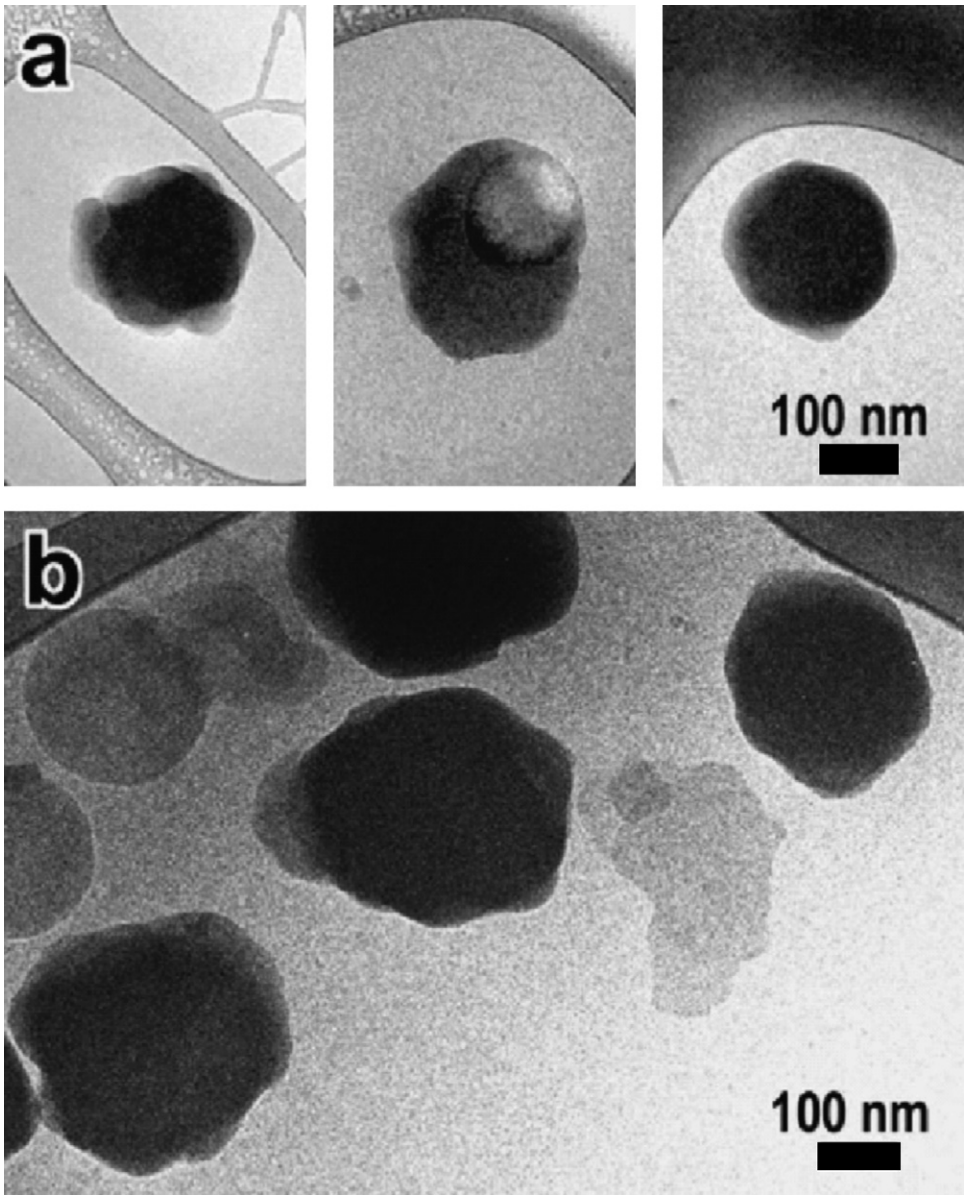

Fig. 11. Cryo-TEM images of nanospheres made from (a) β-CD(C_8F_{17})$_4$, (b) β-CD(C_6F_{13})$_7$, embedded in vitreous ice. Reprinted from Péroche et al. (2005).

ends of the axis (Wenz et al., 2006). If a rotaxane has more than two rings, it is called polyrotaxane. Pseudorotaxane is referred to a rotaxane without stoppers and so is pseudopolyrotaxane.

There are three different approaches for the synthesis of rotaxanes, two of which are currently available for cyclodextrin rotaxanes as shown in Fig. 14 (left). The first one is so-called ''threading'' approach, in which bulky substituents are attached to both ends of the included axis molecule, then the stoppers are coupled to the threaded axis through so-called ''rotaxanation reaction''. The second one is called ''slippage'' in which cyclodextrin rings are threaded over a dumbbell, which mostly leads to pseudorotaxanes. A third hypothetical method, called ''clipping'' approach, is a ring closure of an acyclic maltooligosaccharide around a dumbbell.

A linear cyclodextrin pseudopolyrotaxane is obtained through either threading many cyclodextrin rings onto a polymer chain or polymerizing monomeric axial cyclodextrin inclusion complexes. However, pseudopolyrotaxanes are not kinetically stable, because the cyclodextrin beads can thread off the polymer chain. Polyrotaxanes are synthesized by the attachment of stoppers to pseudopolyrotaxanes at the chain end, within the chain, or along the chain (Fig. 14, right) (Wenz et al., 2006). The stoppers should be not only large enough to block cyclodextrin rings, but also hydrophilic enough to avoid aggregation or precipitation of the polyrotaxanes. The syntheses and properties of rotaxanes and pseudorotaxanes published over the last several years are summarized by Wenz et al. (2006) and by Harada (2001). Work prior to 1998, including work on cyclodextrin catenanes, has been summarized by Nepogodiev and Stoddart (1998).

Much characterization work has been carried out to confirm the characteristic of the rotaxane formed by polymeric glycols and CDs; however, confirmatory structural information is still lacking except for the single crystal X-ray

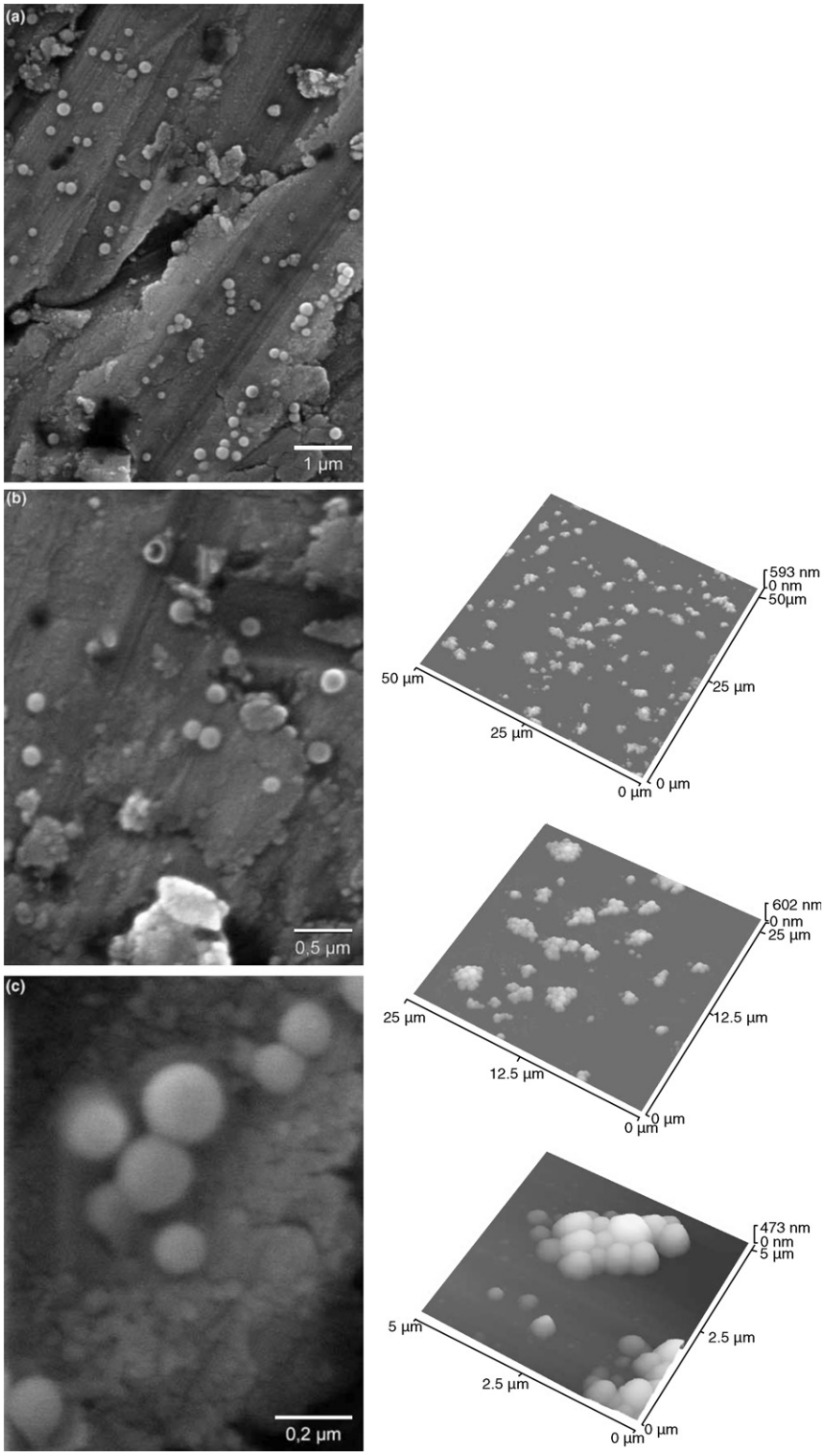

Fig. 12. Left: SEM images of the β-CD21C6 derived solid lipid nanoparticles, scale bar: (a) 1 μm, (b) 0.5 μm and (c) 0.2 μm. Right: Non-contact mode AFM images of the β-CD21C6 derived solid lipid nanoparticles at scan ranges of: (a) 50 μm, (b) 25 μm and (c) 5 μm. Reprinted from Dubes et al. (2003).

structure of PEG-α-CD (Udachin et al., 2000). Herein, we mainly focus on the use of microscopy for characterizing this type of cyclodextrin aggregate. Using microscopic methods such as TEM, AFM, and STM, (pseudo)polyrotaxane chains of the channel type can be directly visualized because they are rather stiff and often rod-like due to the hydrogen bonds between threaded CDs.

A ‘‘molecular abacus’’ based on polyrotaxane, consisting of α-CD rings and PEG chain, was prepared, which was a milestone in the development of molecular devices. Through

Fig. 13. 215 nm × 215 nm raw data AFM image (tapping mode) of retinal-β-CD complex deposited on a silicon (1 0 0) wafer. The bar indicates 100 nm. Reprinted from Botella et al. (1996).

STM, single α-CD rings threading on the PEG chain were detected and manipulated reversibly with the probe of STM because the α-CDs were non-covalently bound to PEG (see Fig. 15) (Shigekawa et al., 2000).

Two novel bis(pseudopolyrotaxane)s composed of metallo-bridged bis(cyclodextrin)s possessing the ligated copper(II) center and polymer chains were synthesized by Liu et al. (2002c). The nanostructured supramolecular aggregates were characterized with STM and TEM. When samples for TEM were prepared, one drop of the solution of bis(pseudopolyrotaxane)s was placed onto a carbon-coated copper grid, and then chromium was shaded to thicken the drop and make the images clearer. The disadvantage of this preparation of samples is that the width of the assembly could not be calculated from TEM images.

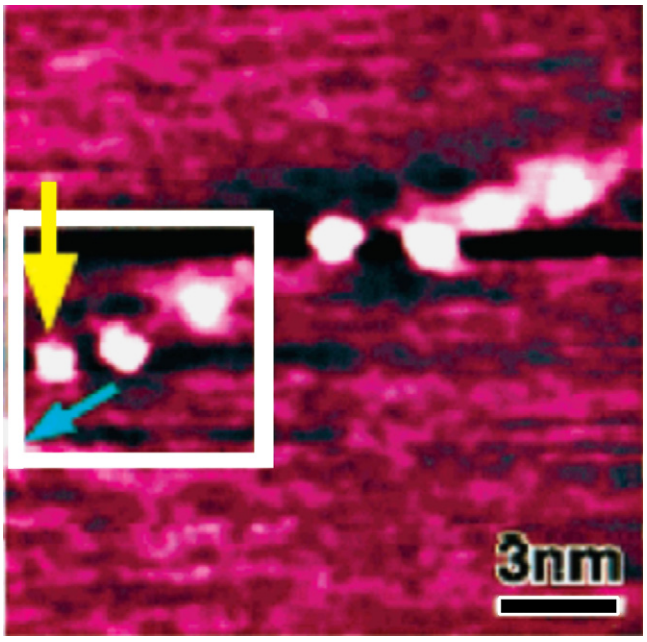

Fig. 15. STM picture of a single α-CD-PEO polyrotaxane; single α-CD and the whole polyrotaxane are visible. Reprinted from Shigekawa et al. (2000).

A polymeric rotaxane constructed from the inclusion complex of β-CD and 4,4′-dipyridine by coordination with nickel(II) ions was synthesized (Liu et al., 2003c). When preparing samples for TEM, unlike above method, a palladium–iridium alloy was applied to thicken the drop and make the images clearer. A rod-like molecular assembly with a length of approximately 450 nm was observed from the TEM micrograph (see Fig. 16). Using STM, a regular arrangement of chains of supramolecules on a graphite substrate was found. Single β-CD unit (a bright dot in STM image) was also clearly shown.

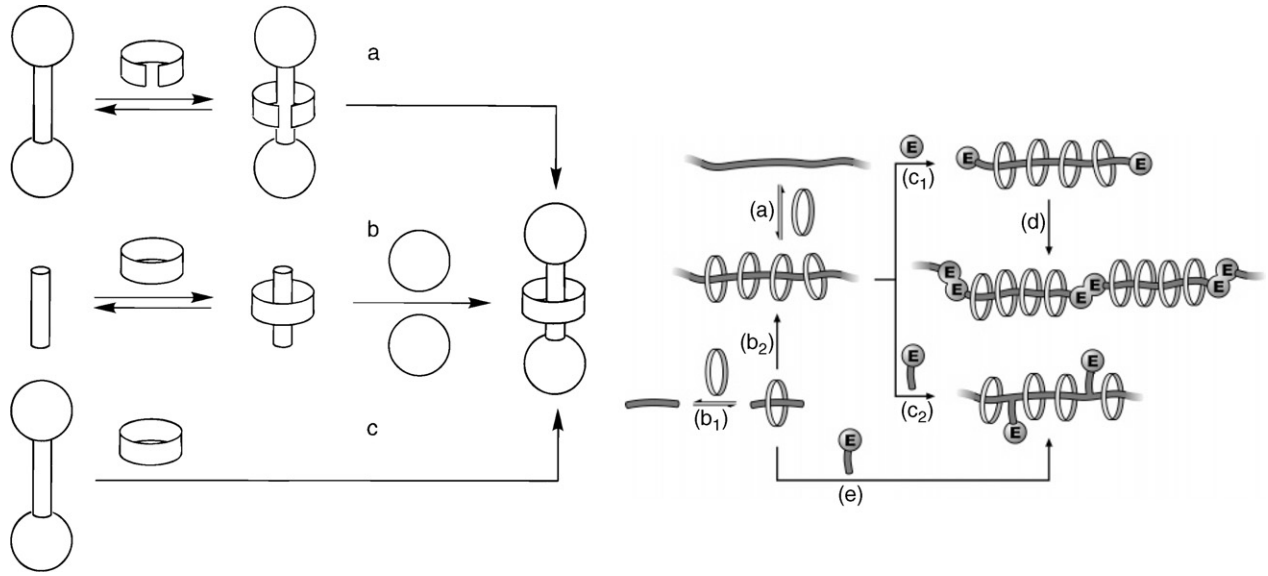

Fig. 14. Left: Three different approaches to the construction of rotaxanes: (a) "clipping"; (b) "threading"; (c) "slippage". Reprinted from Nepogodiev and Stoddart (1998). Right: Possible pathway for the synthesis of polyrotaxanes. *E* = end group. Reprinted from Wenz et al. (2006).

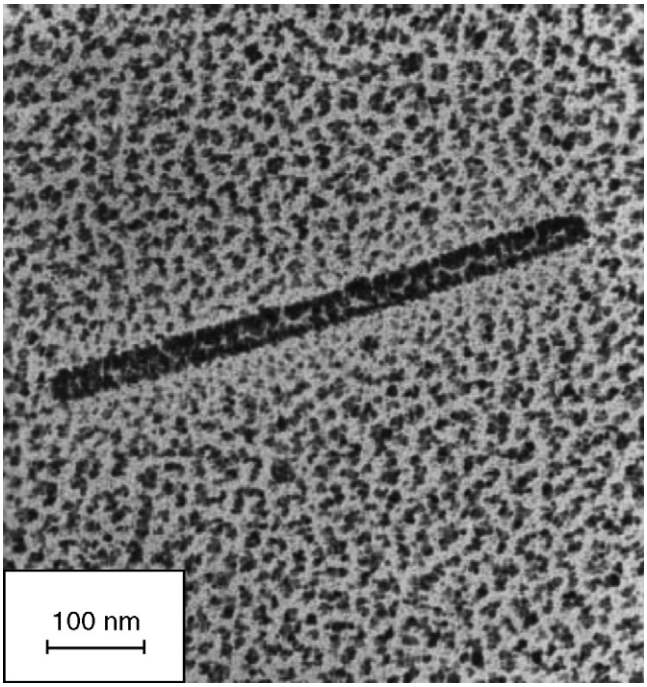

Fig. 16. TEM image of polymeric rotaxane. Reprinted from Liu et al. (2003c).

In another case, one β-CD unit was also detected with STM by Liu et al. They constructed a nanometer-sized cyclodextrin–porphyrin–fullerene aggregate with an interlocked bis-(polyrotaxanes) structure from cyclodextrin–porphyrin conjugate and C60, which exhibited significant chiral and electrochemical properties and would be applied in many fields of chemistry and biology (Liu et al., 2005a). STM images give a fine structure of the aggregate, and it can be seen that the linear structure shown in TEM image (see Fig. 17, left) is actually an ordered double-lined array (total width 3.5 nm measured by STM) composed of many bright dots. One bright dot corresponds to one β-CD unit (see Fig. 17, right).

A series of conjugated polyrotaxane with β-CDs as rings through Suzuki coupling as the polymerization reaction was developed successfully with a high threaded poly(*para*-phenylene) (PPP), PF (polyfluorene), and PDV (poly(diphenylene-vinylene)) (Cacialli et al., 2002). To obtain more direct evidence of the different aggregation behaviors, Tapping Mode Scanning Force Microscopy (TM-SFM) of ultra-thin films, spin-coated on muscovite mica substrates was employed. Fig. 18a shows the β-CD-PPP polyrotaxanes with individual molecular rods which are distinguished from one another. Fig. 18b displays an isolated anisotropic nanostructure of β-CD-PPP spin-coated on mica from a dilute solution (Cacialli et al., 2002). Other (pseudo)polyrotaxane chains can also be directly visualized by microscopic methods such as SEM (Liu et al., 2002a; Ogoshi and Chujo, 2003), TEM (Cheng et al., 2005; Liu et al., 2002a), AFM (Loethen et al., 2006; Shinohara et al., 2006; van den Boogaard et al., 2004), and STM (Liu et al., 2003b, 2002a, 2004a,c; Yoshida et al., 1999).

5. Cyclodextrin nanotubes and their secondary assembly

5.1. Cyclodextrin nanotubes

According to the interaction fashion between two adjacent CDs, cyclodextrin nanotubes include two types: cyclodextrin molecular tubes in which two adjacent CDs are associated by covalent bond and common cyclodextrin nanotubes in which two adjacent CDs are associated by non-covalent bond such as hydrogen bond. Based on the polyrotaxanes, cyclodextrin molecular tube consisting of about fifteen multiply bridged α-CD units was first synthesized from threaded cyclodextrins (Harada et al., 1993). A novel bis(molecular tube)s, consisting of organoselenium-bridged β-CD and platinum(IV) ion, was also fabricated via the pseudorotaxane with poly(propylene glycol) (Y. Liu et al., 2001). The molecular tube has been applied to improving the refolding yields of several enzymes (Yazdanparast et al., 2006), and can selectively include guests to form inclusion complexes (Ikeda et al., 2001, 2000; Kalashnikov et al., 2004; Samitsu et al., 2004).

Through potential-controlled adsorption technology, Ohira et al. constructed nanotube structures of α-, β-, and γ-CDs without using a threaded polymer, onto Au(1 1 1) surfaces in sodium perchlorate solution (Ohira et al., 2003). The typical STM images shows the adsorption behaviors including the formation of nanotube structures of CDs depends on the electrode potential (see Fig. 19). Furthermore, details of the adsorption behaviors of α-, β-, and γ-CDs on Au(1 1 1) were described with the observation of dynamic processes, such as self-ordering, order-to-disorder, and order-to-desorption.

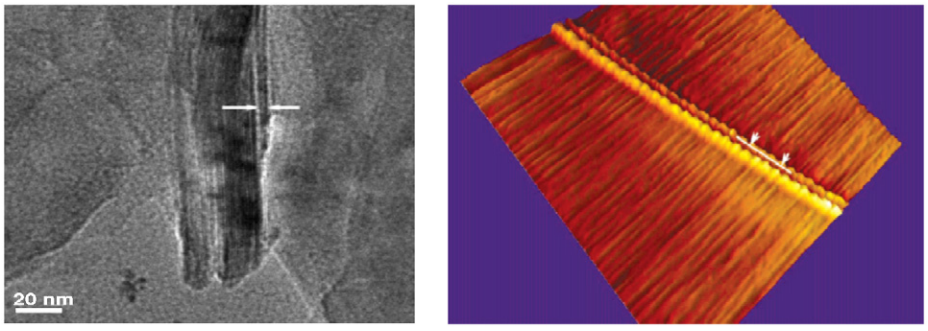

Fig. 17. Left: TEM images of the aggregates. Right: STM image of bis-(polyrotaxane) structure on HOPG surface (tunneling current 1.0 nA). Reprinted from Liu et al. (2005a).

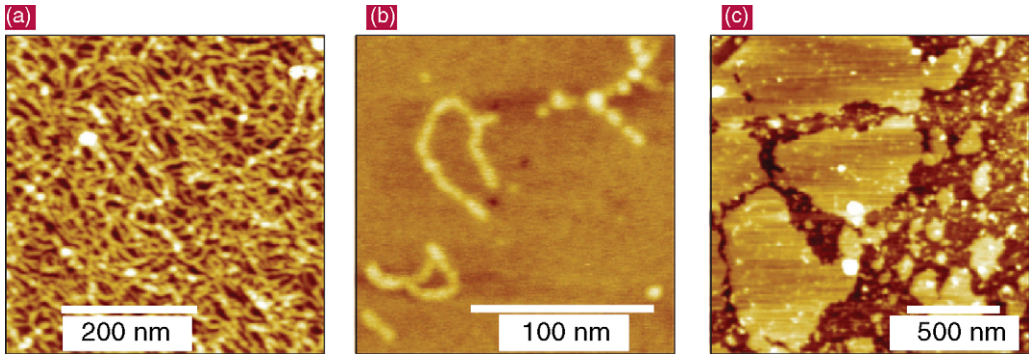

Fig. 18. Surface morphology of spin-coated polyrotaxanes and reference polymer. Tapping mode SFM images of β-CD-PPP (a, b),and unthreaded PPP (c) films spin-coated from a Millipore water solution on a mica substrate. The average degree of polymerization is $N = 10$ (a and c) and $N \approx 20$–30 (b), leading to average contour lengths along the extended rod-like chains of about 17 nm and 30–50 nm. They estimate a corrected rod width of ∼1.6 nm and height of 0.4 ± 0.1 nm. The self-assembled monolayers shown in (c) exhibit holes with constant depths. The vertical scale is 4 nm (a), 3 nm (b), and 10 nm (c). Reprinted from Cacialli et al. (2002).

Cyclodextrin nanotubes can also be induced by organic molecules. Agbaria and Gill discovered that 2,5-diphenyloxazole (PPO) molecule could lead to the formation of a coaxial array of γ-CD beads in aqueous solutions (Agbaria and Gill, 1988). Later, they found some other oxazole molecules, such as 2,5-diphenyl 1,3,4-oxadiazole (PPD), 2-phenyl-5-(4-diphenyl) 1,3,4-oxadiazole (PBD), 2,5-(4,4′-diphenyl) 1,3,4-oxazole (BBOD) can also form nanotubes with γ-CD (Agbaria and Gill, 1994). Li et al. reported on the formation of rigid molecular nanotube aggregates of β-CD and γ-CD through

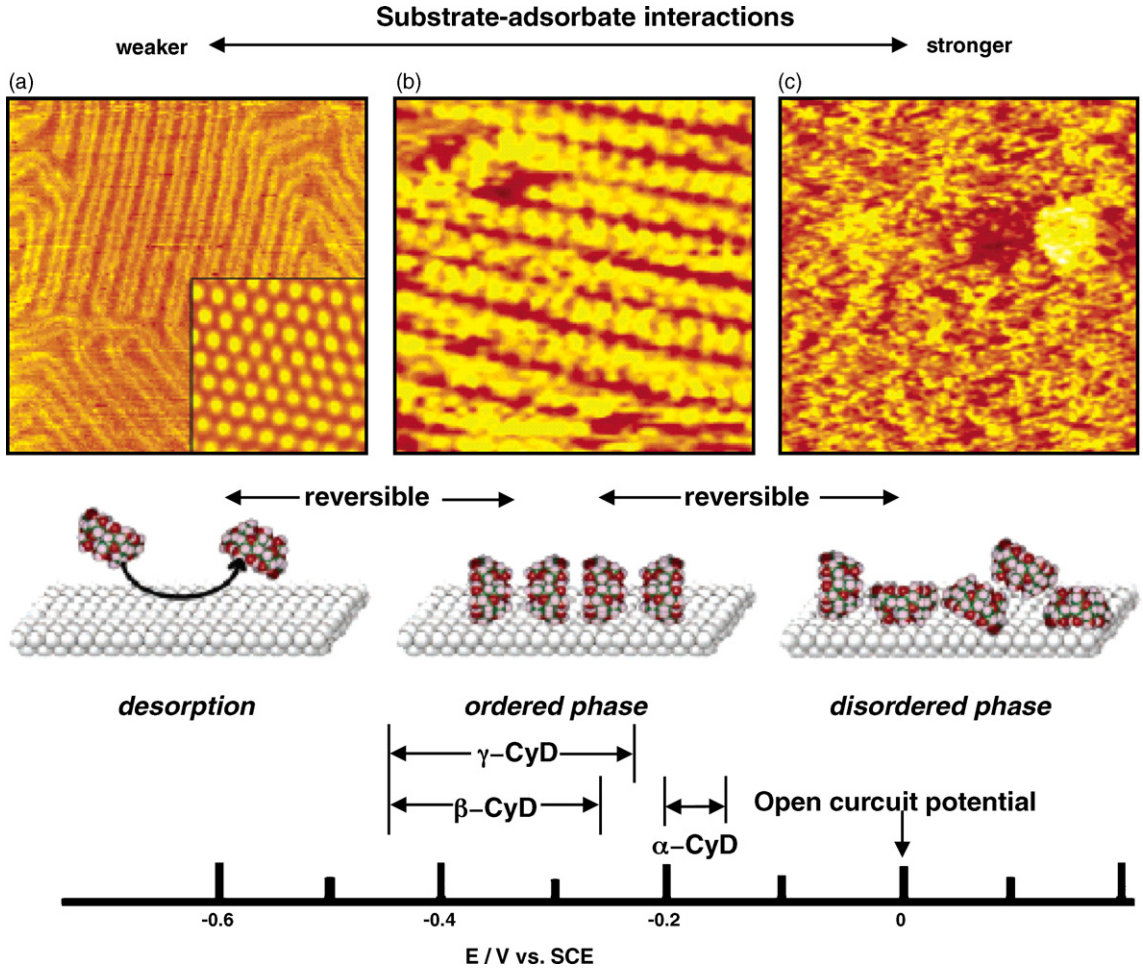

Fig. 19. Electrode potential diagram for three states: (a) "desorption" state, (b) "ordered state", and (c) "disordered state", with corresponding schematic illustrations and typical STM images. (a) Tunneling current, I_t: 2.4 nA; tip potential, E_t: +0.14 V; and the electrode potential, E_s: −0.60 V. (b) I_t: 2.4 nA, E_t: +0.14 V, and E_s: −0.45 V. (c) I_t: 1.6 nA, E_t: −0.13 V, and E_s: +0.10 V. Each AISO potential range for the nanotubes formation of α-, β-, and γ-CD is marked by the arrow. Reprinted from Ohira et al. (2003).

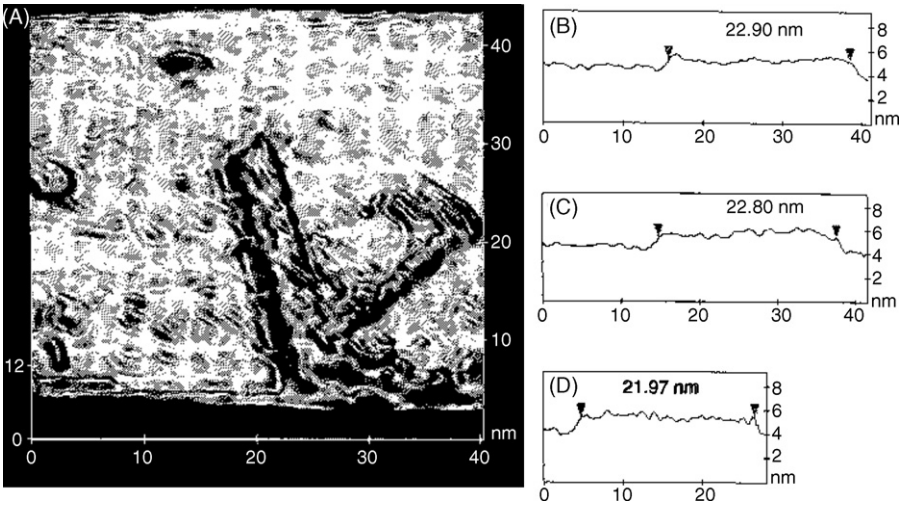

Fig. 20. DPH-β-CD nanotube aggregates imaged by STM. One drop of the solution was deposited on a highly ordered pyrolytic graphite (HOPG) substrate and dried at least 2 h. A Nanoscope II scanning tunneling microscope (Digital Instruments) with head type A and a Pt–Ir wire tip was used in the constant height mode with a set point of 0.25 nA and a basis of 197.75 mV. The image was filtered to remove some noise. (A) Three DPH-β-CD nanotubes, two together and one individual (rods 1, 2, and 3, from left to right). (B–D) The cross-sections along rods 1, 2, and 3, respectively, and their length. The other images may be free CD molecules or clusters. Reprinted from Li and McGown (1994).

linkage by the rodlike molecules of all-*trans*-1,6-diphenyl-1,3,5-hexatriene (DPH). Furthermore, the visualized images of nanotubes were obtained with STM (see Fig. 20) (Li and McGown, 1994). After that, the investigation on cyclodextrin nanotubes induced by organic molecules has been received increasing interest in recent years. Pistolis et al. gave a detailed study on the size effect of the homologues of the α,ω-diphenylpolyebes series, with two, three and four double bonds, on the formation of nanotubes with γ-CD (Pistolis and Malliaris, 1996, 1998). Also, Roy et al. found γ-CD formed large linear nanotube aggregates under the existence of coumarin 153 in which more than 53 γ-CD units were present (Roy et al., 2005). Wen et al. (2004) reported on the nanotube formation in solution between β-CD and cinchonine.

Our research group is interested in the studies concerning the formation of cyclodextrin nanotubes induced by organic molecules and aims to find out what kinds of organic molecules can benefit the formation of cyclodextrin nanotube. So far, we have found some molecules such as 2-phenyl-5-(4-diphenylyl) 1,3,4-oxadiazole (PBD) (Wu et al., 2006c; Zhang et al., 2002), butyl-PBD (Zhang et al., 2002), 2,2′-biquinoline (BQ) (Zhang et al., 2003), 1,1′-(methylenedi-1,4-phenylene) bismaleimide (MDP-BMI) (Zhang et al., 2003), 4,4′-bis(2-benzoxazolyl) stilbene (BOS) (Wu et al., 2006a), *N*,*N*′-dipenylbenzidine (DPB) (Wu et al., 2006b), and 2,2′-*p*-phenylenebis (5-phenyloxazole) (POPOP) (Cheng et al., 2006) could form nanotubes with CDs. When the pH value of the system of cyclodextrin nanotube rose above 12, the nanotubes were disassembled owing to ionization of the hydroxyl groups on CDs (Wu et al., 2006b). It was also found that the presence of 0.5 M urea or 10% (v/v) DMF would make nanotubes decompose (Wu et al., 2006c). At high temperature, the similar phenomenon would happen (Wu et al., 2006b). According to the above results, we summarized the following elementary rule for the formation of nanotubes induced by organic molecules: (1) the hydrophobic interaction between CDs and organic molecules; (2) hydrogen bonding between the adjacent CDs; (3) organic molecules with appropriate size and good rigidity; (4) thermodynamic stability (higher temperature would make nanotubes break down); (5) β- and γ-CDs but not α-CD are able to form nanotubes in the presence of organic molecules (Wu, 2006).

5.2. The secondary assembly of cyclodextrin nanotubes

Using fluorescence microscopy we found the rods with the length of 2.0–5.0 μm in the system of PBD and β-CD as shown in Fig. 21, where the rods are bright relative to the background (Wu et al., 2006c). These rods were also observed with TEM as shown in Fig. 22a. A high-resolution TEM micrograph shows

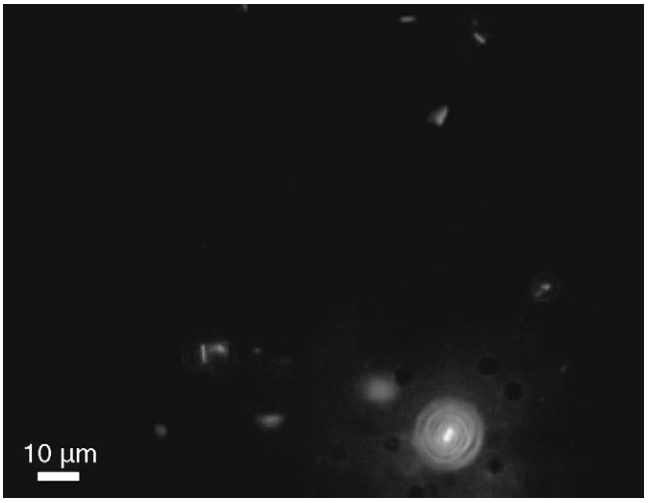

Fig. 21. Fluorescence image of the micrometer-sized rodlike structure of PBD–β-CD nanotube aggregates. [PBD] = 1×10^{-5} M, [β-CD] = 10 mM. Reprinted from Wu et al. (2006c).

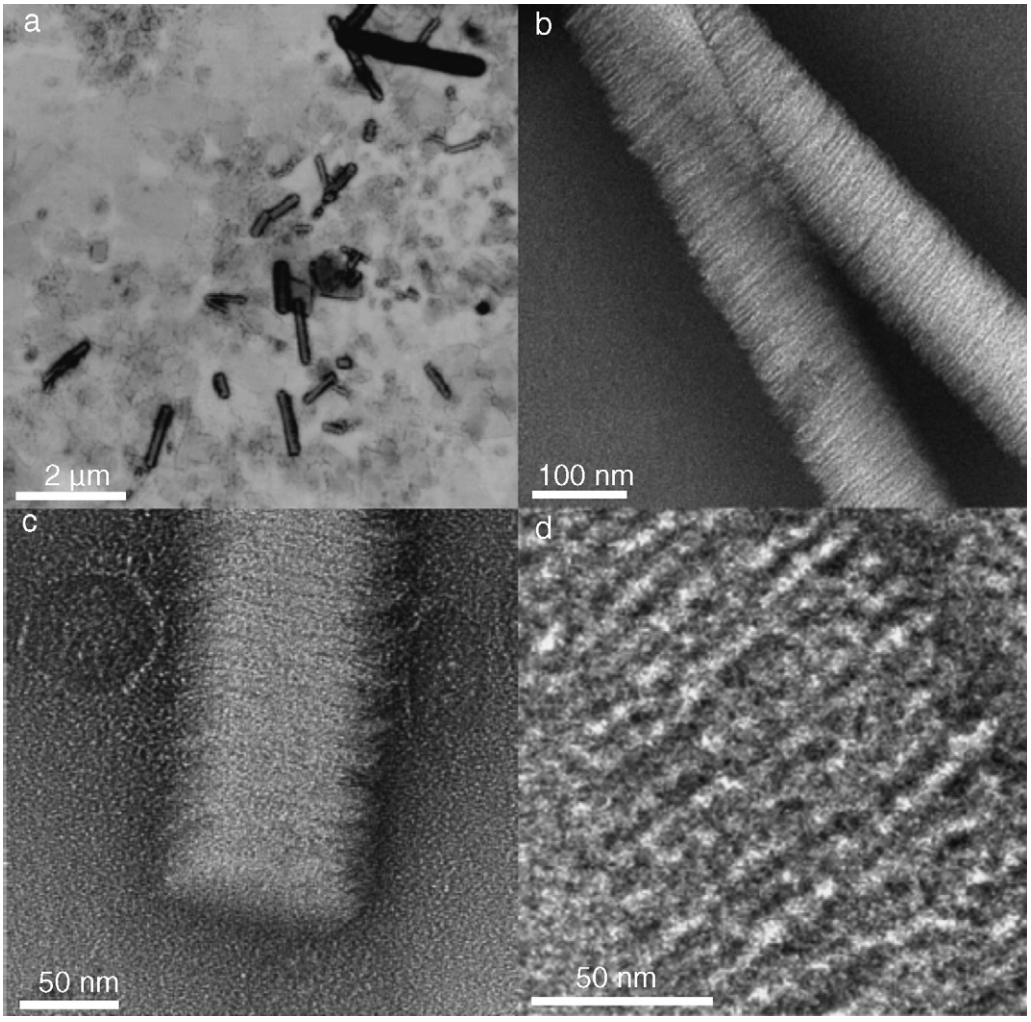

Fig. 22. TEM (a) and high-resolution TEM (b) micrographs of the micrometer-sized rodlike structure of PBD-β-CD nanotube; high-resolution TEM micrographs of the section (c) and the surface (d) of the rod. [PBD] = 1×10^{-5} M, [β-CD] = 10 mM. Reprinted from Wu et al. (2006c).

that the rod as a whole is actually assembled by thousands of smaller nanotubes in a stack way layer by layer (see Fig. 22b). Fig. 22c provides important information about the dimensions of the rods, that is, the section of the rod is approximately oblong and the thickness of the rod is about 40 nm. Fig. 22b and c shows that the nanotubes can assemble in three dimensions, two of which seem to be favored over the third, as when bricks are used to construct a wall, resulting in micrometer-sized rods with variable width and length, but constant thickness. The similar phenomenon was also found to the DPB-γ-CD system (Wu et al., 2006b). Comparing to PBD-α-CD system, DLS result of PBD-β-CD system shows appearance of a new peak with mean hydrodynamic radius around 11 nm which corresponds to the size of nanotube other than monomeric and self-aggregated CDs. The system in which the secondary assembly of PBD-β-CD nanotube happened was filtrated and the density measurement of the filtrate indicated that only 60% of CDs were remained in the filtration. Thus, we proposed a novel mechanism of secondary assembly of cyclodextrin nanotube: the solid nanotubes, as the crystal core, induced hollow CDs to grow and aggregate around themselves. Furthermore, the addition of urea and DMF resulted in disassembly of cyclodextrin nanotube and the secondary assembly. At high temperature or high pH value the similar phenomena also happened. However, cyclodextrin nanotube can stably exist in the aqueous solution of 0.5 M NaCl (Wu et al., 2006c). Combining other experimental results, we proposed that the most important driven force of the formation of cyclodextrin nanotubes and their secondary assembly is the hydrogen bonding between CDs (Wu et al., 2006c).

6. Other high-order aggregates of cyclodextrins

Besides the above mentioned aggregates of cyclodextrin, other high-order aggregates of cyclodextrin, such as nanometer structural wire-shaped aggregates (Liu et al., 2002b, 2004b), nanospheres (Hou et al., 2005), polymeric micelles (Wang and Jiang, 2006), network aggregates (J. Liu et al., 2001; Liu et al., 2005b,c), starpolymers (Okumura et al., 2000), bundle shape (Liu et al., 2006), self-assembled multilayer (Crespo-Biel et al., 2005), and cyclic daisy chains (Hoshino et al., 2000) were also reported.

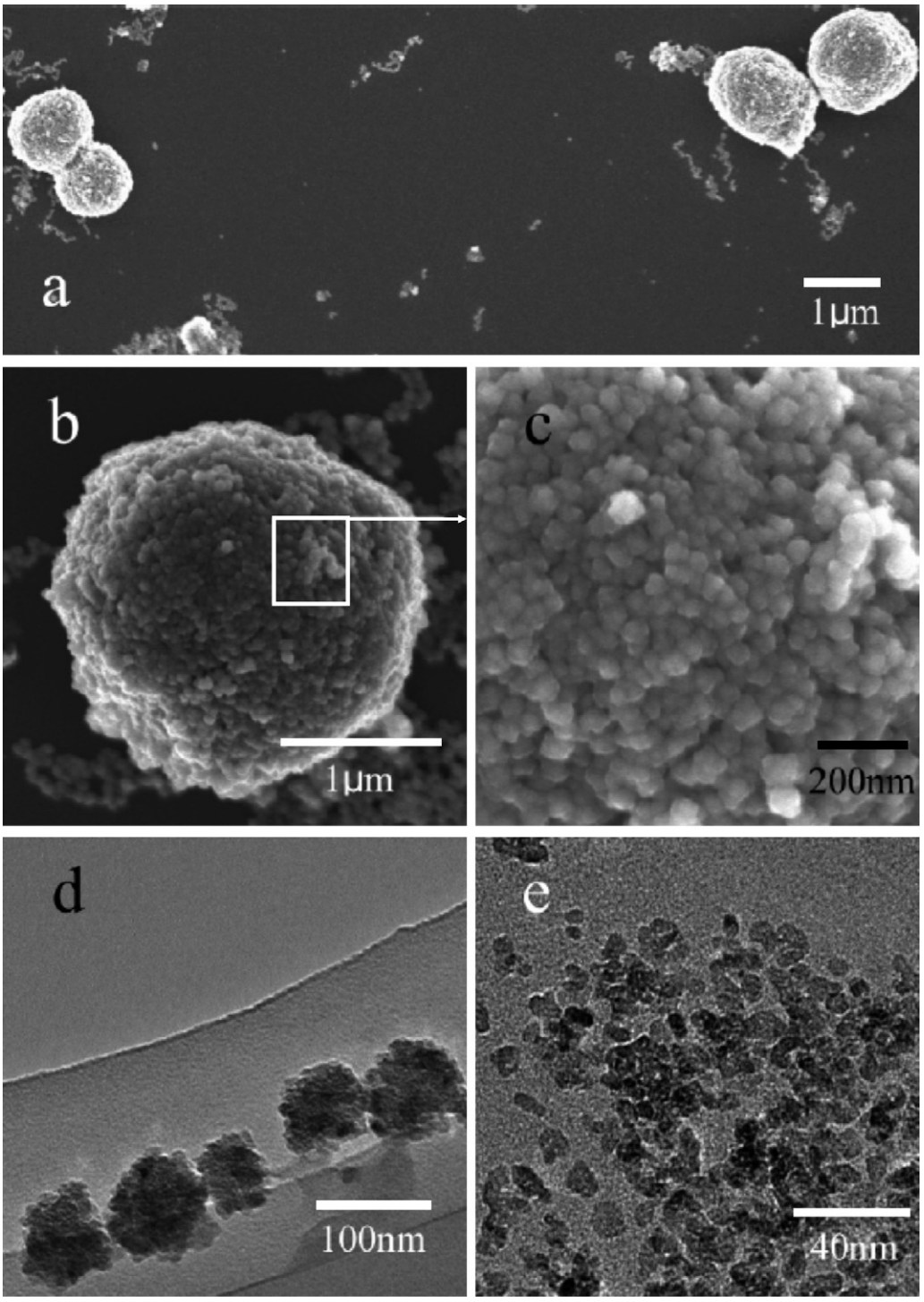

Fig. 23. SEM images (a–c) of sample synthesized from β-CD, oleic acid and oleylamine, TEM image (d) of sample synthesized from only β-CD, and TEM image (e) of sample synthesized from oleic acid and oleylamine. Reprinted from Hou et al. (2005).

Hou et al. (2005) reported on a size-controlled 3D magnetic nanosphere, using β-CD as surfactants, oleic acid and oleylamine as cosurfactants for the assembly of magnetite nanoparticles. Fig. 23 shows SEM and TEM images of the samples stabilized with different amounts of β-CD. Fig. 23a is a SEM image of assembled magnetite prepared at higher temperatures, which has a regular spherical structure with the average size of 2 μm. The enlarged SEM images (Fig. 23b and c) show that the spheres consist of many nanoparticles. In above preparation process, if β-CD but not oleic acid and oleylamine existed, semispherical morphology were obtained (Fig. 23d). If oleic acid and oleylamine but not β-CD existed, isolated particles with an average size of 11 nm were synthesized (Fig. 23e). The above results suggest that the assembly and size of magnetite particles are dependent on the amount of β-CD (Hou et al., 2005).

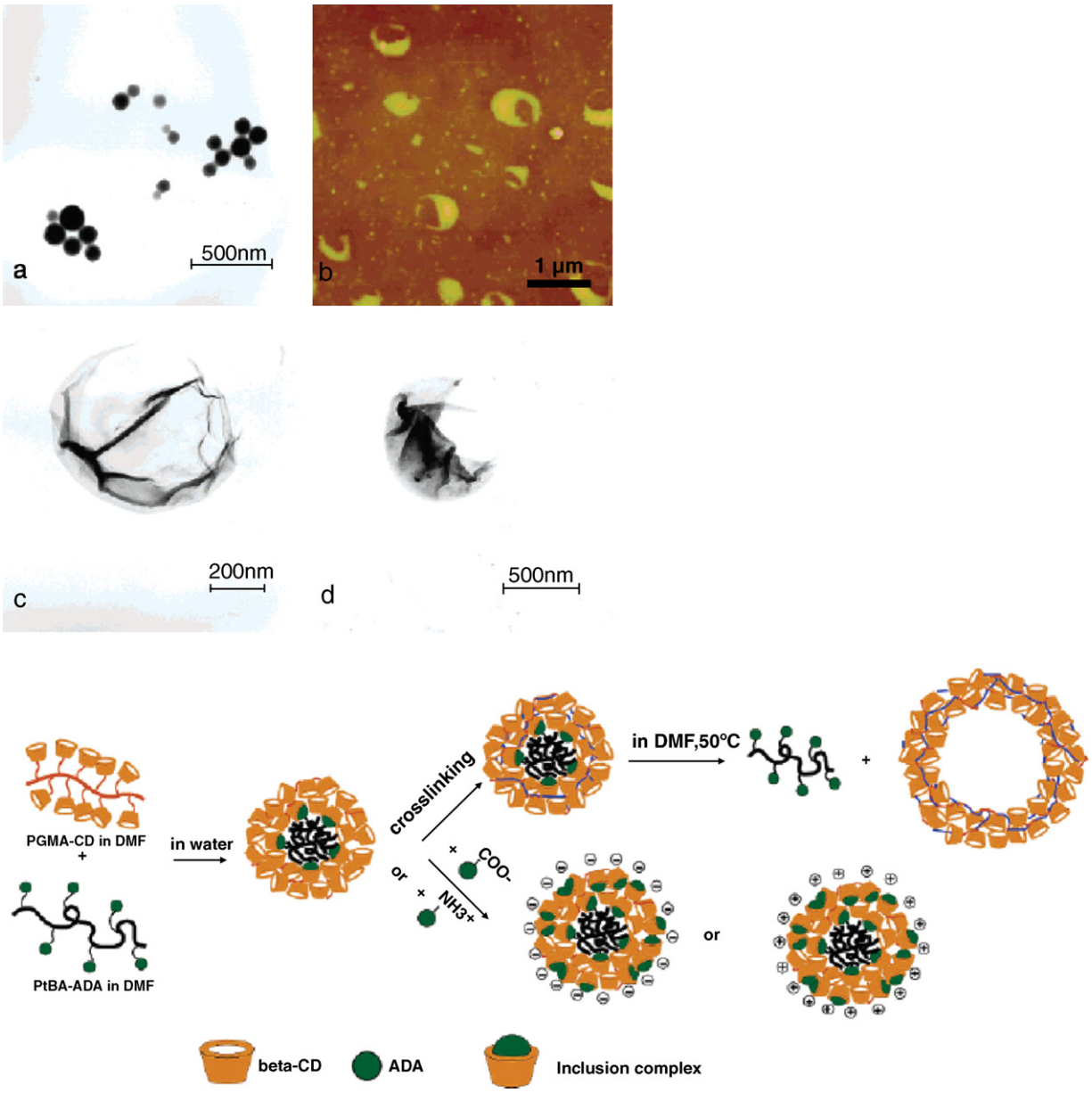

Fig. 24. Top: TEM (a) image of cross-linked micelles M3 and AFM (b) and TEM (c and d) images of the corresponding hollow spheres. Down: An illustration of PGMA-CD/PtBA-ADA micelles and their characters. Reprinted from Wang and Jiang (2006).

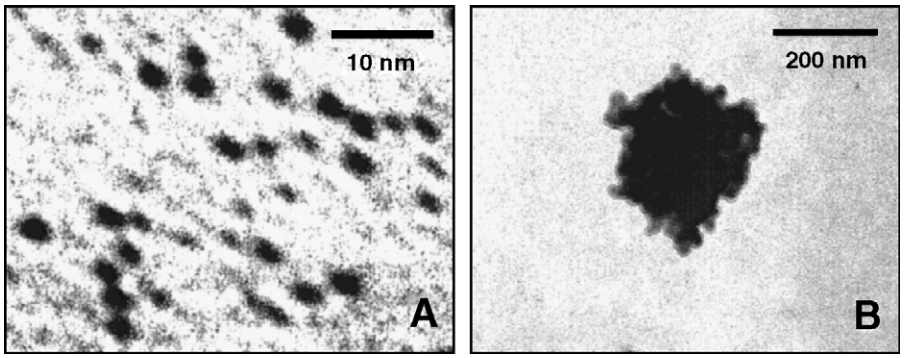

Fig. 25. TEM images of (A) γ-CD-capped gold nanoparticles and (B) C60-induced aggregate. Reprinted from J. Liu et al. (2001).

Wang et al. reported on polymeric micelles, using the inclusion complexation between β-CD and adamantyl group as a driving force (Wang and Jiang, 2006). Via shell cross-linking and core removal of the micelles, hollow spheres composed of β-CD-containing polymers were obtained. These hollow spheres possessed multiscale holes, i.e., the large central one at a size of submicrometers and many small β-CD cavities at 0.7 nm. As shown in the AFM and TEM images (Fig. 24), the morphology of the cross-linked micelles does not change in shape and size while dramatic changes took place when the micellar core was removed: discrete and collapsed hollow spheres in a size range of about 500–1000 nm were formed.

Large network aggregates were formed from water-soluble gold nanoparticles capped with thiolated γ-CD hosts in the presence of C60 fullerene molecules. This aggregation phenomenon was driven by the formation of inclusion complexes between two CDs attached to different nanoparticles and one molecule of C60 (J. Liu et al., 2001). As can be seen from the TEM images in Fig. 25 the addition of C60 makes the γ-CD-capped gold nanoparticles (3.2 nm) to transform into large network aggregates (300 nm).

Another netlike supramolecular aggregates were synthesized through the linkage of gold nanoparticles with cyclodextrin-based polypseudorotaxanes (Liu et al., 2005b,c). TEM images

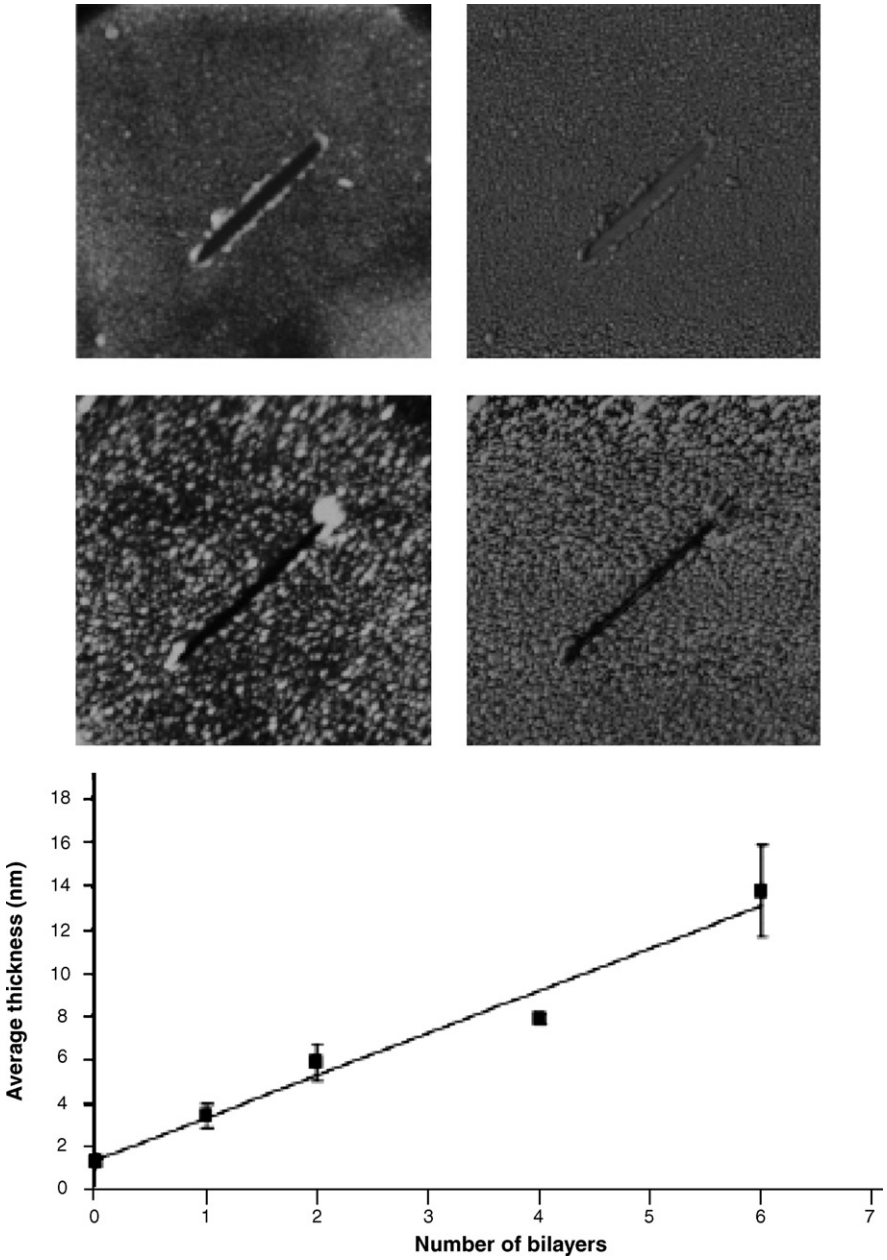

Fig. 26. TM-AFM height (top left, z range 20.0 nm; center left, z range 10.0 nm) and phase (top right, z range 50.0; center right, z range 80.0) images ($\times 1.2\ \mu m^2$) in air of one bilayer (top) and four bilayers (center) on a cyclodextrin self-assembled monolayer after layer-by-layer assembly (0.01 mM in hydrophobic moieties in a 1 mM cyclodextrin pH 2 solution, and cyclodextrin Au nanoparticles, 5.8 μM in water). Bottom: Multilayer thickness as a function of the number of bilayers measured with AFM scratching experiments (Crespo-Biel et al., 2005).

were employed to characterize the sole gold nanoparticles and the further aggregates with polypseudorotaxanes.

A novel kind of self-assembled organic/inorganic multilayers based on multivalent supramolecular interactions between guest-functionalized dendrimers and host-modified gold nanoparticles has been reported by Crespo-Biel et al. (Crespo-Biel et al., 2005). AFM was used for a direct determination of the thickness of the multilayer thin film (Fig. 26). The AFM tip was used to create a scratch down to the gold, and the thickness was determined by scanning across the scratch with the AFM tip. The AFM images show well-defined multilayer formation, an accurate thickness control, and the need of specific host–guest interactions.

7. Conclusions

Cyclodextrins can form different aggregates under different condition. In this review, we have discussed the aggregates of native CDs and modified CDs, inclusion complexes and their aggregates of CDs, cyclodextrin rotaxanes and polyrotaxanes, cyclodextrin nanotubes and their secondary assembly, and other high-order aggregates of CDs. Microscopy, as one of the most important tools to characterize above assembly, has been used widely. It affords a convenient approach to characterize various types of aggregates with size from less than 1 nm to about several micrometers. Not only the large cyclodextrin aggregates but also single cyclodextrin such as α- and β-CDs can be visualized with microscopy tools such as STM. Furthermore, using microscopy instruments such as AFM, single cyclodextrin can be easily manipulated. With the development of microscopy, cyclodextrin aggregates will be investigated more and more widely.

Acknowledgment

This work was supported by the National Natural Science Foundation of China (Grant No. 90206020).

References

Agbaria, R.A., Gill, D., 1988. Extended 2,5-diphenyloxazole-γ-cyclodextrin aggregates emitting 2,5-diphenyloxazole excimer fluorescence. J. Physical Chem. 92, 1052–1055.

Agbaria, R.A., Gill, D., 1994. Non-covalent polymers of oxadiazole derivatives induced by γ-CD in aqueous solution-fluorescence study. J. Photochem. Photobiol. A: Chem. 78, 161–167.

Ariga, K., Kunitake, T., 2006. Supramolecular Chemistry—Fundamentals and Applications. Springer, New York.

Auzely-Velty, R., Djedaini-Pilard, F., Desert, S., Perly, B., Zemb, T., 2000. Micellization of hydrophobically modified cyclodextrins. 1. Micellar structure. Langmuir 16 (8), 3727–3734.

Avakyan, V.G., Nazarov, V.B., Alfimov, M.V., Bagatur'yants, A.A., 1999. Structure of guest–host complexes of beta-cyclodextrin with arenes: a quantum–chemical study. Russ. Chem. Bull. 48 (10), 1833–1844.

Azaroual-Bellanger, N., Perly, B., 1994. Investigation of the dynamics of cyclodextrins and their inclusion complexes in water by deuterium NMR. Magn. Reson. Chem. 32 (1), 8–11.

Becheri, A., Lo Nostro, P., Ninham, B.W., Baglioni, P., 2003. The curious world of polypseudorotaxanes: cyclodextrins as probes of water structure. J. Physical Chem. B 107 (16), 3979–3987.

Bonini, M., Rossi, S., Karlsson, G., Almgren, M., Lo Nostro, P., Baglioni, P., 2006. Self-assembly of beta-cyclodextrin in water. Part 1. Cryo-TEM and dynamic and static light scattering. Langmuir 22, 1478–1484.

Botella, S.M., Martin, M.A., delCastillo, B., Menendez, J.C., Vazquez, L., Lerner, D.A., 1996. Analytical applications of retinoid–cyclodextrin inclusion complexes. 1. Characterization of a retinal-beta-cyclodextrin complex. J. Pharmaceut. Biomed. Anal. 14 (8–10), 909–915.

Bügler, J., Sommerdijk, N.A.J.M., Visser, A.J.W.G., van Hoek, A., Nolte, R.J.M., Engbersen, J.F.J., Reinhoudt, D.N., 1999. Interconnective host–guest complexation of beta-cyclodextrin-calix[4]arene couples. J. Am. Chem. Soc. 121 (1), 28–33.

Cacialli, F., Wilson, J.S., Michels, J.J., Daniel, C., Silva, C., Friend, R.H., Severin, N., Samori, P., Rabe, J.P., O'Connell, M.J., Taylor, P.N., Anderson, H.L., 2002. Cyclodextrin-threaded conjugated polyrotaxanes as insulated molecular wires with reduced interstrand interactions. Nat. Mater. 1 (3), 160–164.

Carofiglio, T., Fornasier, R., Lucchini, V., Simonato, L., Tonellato, U., 2000. Synthesis, characterization, and supramolecular properties of a hydrophilic porphyrin-beta-cyclodextrin conjugate. J. Org. Chem. 65 (26), 9013–9021.

Castro, R., Cuadrado, I., Alonso, B., Casado, C.M., Moran, M., Kaifer, A.E., 1997. Multisite inclusion complexation of redox active dendrimer guests. J. Am. Chem. Soc. 119 (24), 5760–5761.

Chen, Y., Xu, T., Shen, X., Gao, H., 2005. Temperature dependence of the inclusion-dissociation behavior of the inclusion complexes between cationic substituted 3H-Indoles and β-cyclodextrin. Design of a novel type of semi-rotaxane. J. Photochem. Photobiol. A: Chem. 173, 42–50.

Cheng, C.X., Tang, R.P., Xi, F., 2005. Preparation and aggregation of polypseudorotaxane from dendronized poly(methacrylate)-poly(ethylene oxide) diblock copolymer and alpha-cyclodextrin. Macromol. Rapid Commun. 26 (9), 744–749.

Cheng, X.L., Wu, A.H., Shen, X.H., He, Y.K., 2006. The formation of cyclodextrin nanotube induced by POPOP molecule. Acta Physico-Chimica Sinica 22 (12), 1466–1472.

Choisnard, L., Gèze, A., Bigan, J.L., Putaux, J.L., Wouessidjewe, D., 2005. Efficient size control of amphiphilic cyclodextrin nanoparticles through a statistical mixture design methodology. J. Pharm. Pharm. Sci. 8 (3), 593–600.

Choisnard, L., Gèze, A., Putaux, J.L., Wong, Y.S., Wouessidjewe, D., 2006. Nanoparticles of beta-cyclodextrin esters obtained by self-assembling of biotransesterified beta-cyclodextrins. Biomacromolecules 7 (2), 515–520.

Clark, J.L., Booth, B.R., Stezowski, J.J., 2001. Molecular recognition in cyclodextrin complexes of amino acid derivatives. 2. A new perturbation: the room-temperature crystallographic structure determination for the *N*-acetyl-*p*-methoxy-L-phenylalanine methyl ester/beta-cyclodextrin complex. J. Am. Chem. Soc. 123 (40), 9889–9895.

Claudy, P., Letoffe, J.M., Germain, P., Bastide, J.P., Bayol, A., Blasquez, S., Rao, R.C., Gonzalez, B., 1991. Physicochemical characterization of cholesterol-beta cyclodextrin inclusion complexes. J. Thermal Anal. 37, 2497–2506.

Coleman, A.W., Nicolis, I., 1992. Aggregation of cyclodextrin: an explanation of the abnormal solubility of beta-cyclodextrin. J. Inclusion Phenomena Mol. Recogn. Chem. 13, 139–143.

Crespo-Biel, O., Dordi, B., Reinhoudt, D.N., Huskens, J., 2005. Supramolecular layer-by-layer assembly alternating adsorptions of guest- and host-functionalized molecules and particles using multivalent supramolecular interactions. J. Am. Chem. Soc. 127, 7594–7600.

Du, X.Z., Zhang, Y., Huang, X.Z., Jiang, Y.B., Li, Y.Q., Chen, G.Z., 1996. Intense room-temperature phosphorescence of 1-bromonaphthalene in organized media of beta-cyclodextrin and triton X-100. Appl. Spectrosc. 50 (10), 1273–1276.

Duan, M.S., Zhao, N., Ossurardottir, I.B., Thorsteinsson, T., Loftsson, T., 2005. Cyclodextrin solubilization of the antibacterial agents triclosan and triclocarban: formation of aggregates and higher-order complexes. Int. J. Pharmaceut. 297 (1–2), 213–222.

Dubes, A., Parrot-Lopez, H., Abdelwahed, W., Degobert, G., Fessi, H., Shahgaldian, P., Coleman, A.W., 2003. Scanning electron microscopy and atomic force microscopy imaging of solid lipid nanoparticles derived from

amphiphilic cyclodextrins. Eur. J. Pharmaceut. Biopharmaceut. 55, 279–282.

Dyck, A.S.M., Kisiel, U., Bohne, C., 2003. Dynamics for the assembly of pyrene-gamma-cyclodextrin host–guest complexes. J. Physical Chem. B 107 (42), 11652–11659.

Falvey, P., Lim, C.W., Darcy, R., Revermann, T., Karst, U., Giesbers, M., Marcelis, A.T.M., Lazar, A., Coleman, A.W., Reinhoudt, D.N., Ravoo, B.J., 2005. Bilayer vesicles of amphiphilic cyclodextrins: host membranes that recognize guest molecules. Chem.: Eur. J. 11 (4), 1171–1180.

Gaitano, G.G., Brown, W., 1997. Inclusion complexes between cyclodextrins and triblock copolymers in aqueous solution: a dynamic and static light-scattering study. J. Physical Chem. 101, 710–719.

Gao, H., Wang, Y.N., Fan, Y.G., Ma, J.B., 2006. Interactions of some modified mono- and bis-β-cyclodextrins with bovine serum albumin. Bioorg. Med. Chem. 14, 131–137.

Gèze, A., Aous, S., Baussanne, I., Putaux, J.L., Defaye, J., Wouessidjewe, D., 2002. Influence of chemical structure of amphiphilic beta-cyclodextrins on their ability to form stable nanoparticles. Int. J. Pharm. 242 (1–2), 301–305.

Gèze, A., Putaux, J.L., Choisnard, L., Jéhan, P., Wouessidjewe, D., 2004. Long-term shelf stability of amphiphilic beta-cyclodextrin nanosphere suspensions monitored by dynamic light scattering and cryo-transmission electron microscopy. J. Microencapsul. 21 (6), 607–613.

Gonzalez-Gaitano, G., Rodriguez, P., Isasi, J.R., Fuentes, M., Tardajos, G., Sanchez, M., 2002. The aggregation of cyclodextrins as studied by photon correlation spectroscopy. J. Inclusion Phenomena Macrocyclic Chem. 44, 101–105.

Greenhall, M.H., Lukes, P., Kataky, R., Agbor, N.E., Badyal, J.P.S., Yarwood, J., Parker, D., Petty, M.C., 1995. Monolayer and multilayer films of cyclodextrins substituted with 2 and 3 alkyl chains. Langmuir 11 (10), 3997–4000.

Hamai, S., 1990. Association modes of a 1:1 inclusion compound of beta-cyclodextrin with 1-cyanonaphthalene in aqueous solutions: self-association, association with alcohols, and association with a 1:1 beta-cyclodextrin-anisole inclusion compound. J. Physical Chem. 94 (6), 2595–2600.

Hamai, S., 1991. Exciple formation between perylene and *N*,*N*-dimethylaniline in a ternary inclusion compound with γ-cyclodextrin in H_2O–ethanol (7:3) mixture. Bull. Chem. Soc. Jpn. 64 (2), 431–438.

Hamai, S., 1996. The excimer fluorescence of 2-methylnaphthalene in beta- and gamma-cyclodextrin aqueous solutions. Bull. Chem. Soc. Jpn. 69 (3), 543–549.

Hamai, S., 2000. Interactions of beta- and gamma-cyclodextrins with thionine and 2-naphthalenesulfonate in aqueous solution. Bull. Chem. Soc. Jpn. 73 (4), 861–866.

Hamai, S., Hatamiya, A., 1996. Excimer formation in inclusion complexes of beta-cyclodextrin with 1-alkylnaphthalenes in aqueous solutions. Bull. Chem. Soc. Jpn. 69 (9), 2469–2476.

Hamelin, B., Jullien, L., Laschewsky, A., du Penhoat, C.H., 1999. Self-assembly of janus cyclodextrins at the air-water interface and in organic solvents. Chem.: Eur. J. 5 (2), 546–556.

Hapiot, F., Tilloy, S., Monflier, E., 2006. Cyclodextrins as supramolecular hosts for organometallic complexes. Chem. Rev. 106, 767–781.

Harada, A., 2001. Cyclodextrin-based molecular machines. Acc. Chem. Res. 34 (6), 456–464.

Harada, A., Li, J., Kamachi, M., 1993. Synthesis of a tubular polymer from threaded cyclodextrins. Nature 364, 516–518.

Hoshino, T., Miyauchi, M., Kawaguchi, Y., Yamaguchi, H., Harada, A., 2000. Daisy chain necklace: tri[2]rotaxane containing cyclodextrins. J. Am. Chem. Soc. 122, 9876–9877.

Hou, Y., Kondoh, H., Shimojo, M., Sako, E.O., Ozaki, N., Kogure, T., Ohta, T., 2005. Inorganic nanocrystal self-assembly via the inclusion interaction of β-cyclodextrins: toward 3D spherical magnetite. J. Physical Chem. B 109 (11), 4845–4852.

Ikeda, T., Ooya, T., Yui, N., 2000. Supramolecular network formation through inclusion complexation of an alpha-cyclodextrin-based molecular tube. Macromol. Rapid Commun. 21 (17), 1257–1262.

Ikeda, T., Hirota, E., Qoya, T., Yui, N., 2001. Thermodynamic analysis of inclusion complexation between alpha-cyclodextrin-based molecular tube and sodium alkyl sulfonate. Langmuir 17 (1), 234–238.

Liu, J., Alvarez, J., Ong, W., Kaifer, A.E., 2001. Network aggregates formed by C-60 and gold nanoparticles capped with gamma-cyclodextrin hosts. Nano Lett. 1 (2), 57–60.

Kakuchi, T., Narumi, A., Matsuda, T., Miura, Y., Sugimoto, N., Satoh, T., Kaga, H., 2003a. Glycoconjugated polymer. 5. Synthesis and characterization of a seven-arm star polystyrene with beta-cyclodextrin core based on TEMPO-mediated living radical polymerisation. Macromolecules 36 (11), 3914–3920.

Kakuchi, T., Narumi, A., Miura, Y., Matsuya, S., Sugimoto, N., Satoh, T., Kaga, H., 2003b. Glycoconjugated polymer. 4. Synthesis and aggregation property of well-defined end-functionalized polystyrene with beta-cyclodextrin. Macromolecules 36 (11), 3909–3913.

Kalashnikov, P.A., Kotel'nikov, G.V., Moiseeva, S.P., Topchieva, I.N., 2004. Inclusion complexes formed by sodium dodecyl sulfate and cyclodextrin-based nanotubes. Colloid J. 66 (5), 542–546.

Kano, K., Takenoshita, I., Ogawa, T., 1982. Fluorescence quenching of pyrene and naphthalene in aqueous cyclodextrin solutions—evidence of 3-component complex formation. J. Physical Chem. 86, 1833–1838.

Li, G., McGown, L.B., 1994. Molecular nanotube aggregates of β- and γ-cyclodextrins linked by diphenylhexatrienes. Science 264, 249–251.

Ling, C.C., Darcy, R., Risse, W., 1993. Cyclodextrin liquid-crystals-synthesis and self-organization of amphiphilic thio-beta-cyclodextrins. J. Chem. Soc.: Chem. Commun. 5, 438–440.

Liu, Y., Li, L., Fan, Z., Zhang, H.Y., Wu, X., Guan, X.D., Liu, S.X., 2002a. Supramolecular aggregates formed by intermolecular inclusion complexation of organo-selenium bridged bis(cyclodextrin)s with calix[4]arene derivative. Org. Lett. 2 (4), 257–261.

Liu, Y., Li, L., Fan, Z., Zhang, H.Y., Wu, X., Guan, X.D., Liu, S.X., 2002b. Supramolecular aggregates formed by intermolecular inclusion complexation of organo-selenium bridged bis(cyclodextrin)s with calix[4]arene derivative. Nano Lett. 2 (4), 257–261.

Liu, Y., Li, L., Zhang, H.Y., Zhao, Y.L., Wu, X., 2002c. Bis(pseudopolyrotaxane)s possessing copper(II) ions formed by different polymer chains and bis(beta-cyclodextrin)s bridged with a 2,2′-bipyridine-4,4′-dicarboxy tether. Macromolecules 35 (27), 9934–9938.

Liu, Y., Fan, Z., Zhang, H.Y., Diao, C.H., 2003a. Binding ability and self-assembly behavior of linear polymeric supramolecules formed by modified beta-cyclodextrin. Org. Lett. 5 (3), 251–254.

Liu, Y., Fan, Z., Zhang, H.Y., Yang, Y.W., Ding, F., Liu, S.X., Wu, X., Wada, T., Inoue, Y., 2003b. Supramolecular self-assemblies of, beta-cyclodextrins with aromatic tethers: factors governing the helical columnar versus linear channel superstructures. J. Org. Chem. 68 (22), 8345–8352.

Liu, Y., Zhao, Y.L., Zhang, H.Y., Song, H.B., 2003c. Polymeric rotaxane constructed from the inclusion complex of beta-cyclodextrin and 4,4′-dipyridine by coordination with nickel(II) ions. Angew. Chem.: Int. Ed. 42 (28), 3260–3263.

Liu, Y., Song, Y., Wang, H., Zhang, H.Y., Li, X.Q., 2004a. Bis(polypseudorotaxane)s formed by multiple metallo-bridged beta-cyclodextrins and the thermodynamic origin of their molecular aggregation. Macromolecules 37 (17), 6370–6375.

Liu, Y., Wang, H., Liang, P., Zhang, H.Y., 2004b. Water-soluble supramolecular fullerene assembly mediated by metallobridged beta-cyclodextrins. Angew. Chem.: Int. Ed. 43 (20), 2690–2694.

Liu, Y., Zhao, Y.L., Zhang, H.Y., Li, X.Y., Liang, P., Zhang, X.Z., Xu, J.J., 2004c. Supramolecular polypseudorotaxane with conjugated polyazomethine prepared directly from two inclusion complexes of beta-cyclodextrin with tolidine and phthaldehyde. Macromolecules 37 (17), 6362–6369.

Liu, Y., Liang, P., Chen, Y., Zhang, Y.M., Zheng, J.Y., Yue, H., 2005a. Interlocked bis(polyrotaxane) of cyclodextrin–porphyrin systems mediated by fullerenes. Macromolecules 38, 9095–9099.

Liu, Y., Wang, H., Chen, Y., Ke, C.F., Liu, M., 2005b. Supramolecular aggregates constructed from gold nanoparticles and L-Try-CD polypseudorotaxanes as captors for fullerenes. J. Am. Chem. Soc. 127 (2), 657–666.

Liu, Y., Zhao, Y.L., Chen, Y., Wang, M., 2005c. Supramolecular assembly of gold nanoparticles mediated by polypseudorotaxane with thiolated beta-cyclodextrin. Macromol. Rapid Commun. 26, 401–406.

Liu, Y., Chen, G.S., Chen, Y., Zhang, N., Chen, J., Zhao, Y.L., 2006. Bundle-shaped cyclodextrin-Tb nano-supramolecular assembly mediated by C60: intramolecular energy transfer. Nano Lett. 6 (10), 2196–2200.

Loethen, S., Ooya, T., Choi, H.S., Yui, N., Thompson, D.H., 2006. Synthesis, characterization, and pH-triggered dethreading of alpha-cyclodextrin-poly(ethylene glycol) polyrotaxanes bearing cleavable endcaps. Biomacromolecules 7 (9), 2501–2506.

Loftsson, T., Masson, M., Brewster, M.E., 2004. Self-association of cyclodextrins and cyclodextrin complexes. J. Pharmaceut. Sci. 93, 1091–1099.

Lombardo, D., Longo, A., Darcy, R., Mazzaglia, A., 2004. Structural properties of nonionic cyclodextrin colloids in water. Langmuir 20 (4), 1057–1064.

Mahalingam, V., Onclin, S., Péter, M., Ravoo, B.J., Huskens, J., Reinhoudt, D.N., 2004. Directed self-assembly of functionalized silica nanoparticles on molecular printboards through multivalent supramolecular interactions. Langmuir 20, 11756–11762.

Mazzaglia, A., Ravoo, B.J., Darcy, R., Gambadauro, P., Mallamace, F., 2002. Aggregation in water of nonionic amphiphilic cyclodextrins with short hydrophobic substituents. Langmuir 18 (5), 1945–1948.

Mazzaglia, A., Forde, D., Garozzo, D., Malvagna, P., Ravoo, B.J., Darcy, R., 2004. Multivalent binding of galactosylated cyclodextrin vesicles to lectin. Org. Biomol. Chem. 2 (7), 957–960.

McAlpine, S.R., Garcia-Garibay, M.A., 1998. Studies of naphthyl-substituted beta-cyclodextrins. Self-aggregation and inclusion of external guests. J. Am. Chem. Soc. 120 (18), 4269–4275.

Mele, A., Mendichi, R., Selva, A., 1998. Non-covalent associations of cyclomaltooligosaccharides (cyclodextrins) with trans-beta-carotene in water: evidence for the formation of large aggregates by light scattering and NMR spectroscopy. Carbohydr. Res. 310 (4), 261–267.

Michels, J.J., Baars, M.W.P.L., Meijer, E.W., Huskens, J., Reinhoudt, D.N., 2000. Well-defined assemblies of adamantyl-terminated poly(propylene imine) dendrimers and beta-cyclodextrin in water. J. Chem. Soc.-Perkin Trans. 2 (9), 1914–1918.

Mytides, P., Rozou, S., Benaki, D., Antoniadou-Vyza, E., 2006. 2,2′:6′2″-Terpyridine [hydroxypropyl-beta-cyclodextrin] 1:3 complex used as chelating agent for the determination of iron with a sensitive, selective and fast liquid chromatographic method. Anal. Chim. Acta 566 (1), 122–129.

Nakahara, H., Tanaka, H., Fukuda, K., Matsumoto, M., Tagaki, W., 1996. Selective inclusion of naphthalene derivatives by monolayers of amphiphilic cyclodextrins at the air–water interface. Thin Solid Films 285, 687–690.

Nakamura, A., Sato, S., Hamasaki, K., Ueno, A., Toda, F., 1995. Association of 1/1 inclusion complexes of cyclodextrins into homodimers and heterodimers – a spectroscopic study using a Tict-forming fluorescent-probe as a guest compound. J. Physical Chem. 99 (27), 10952–10959.

Nepogodiev, S.A., Stoddart, J.F., 1998. Cyclodextrin-based catenanes and rotaxanes. Chem. Rev. 98 (5), 1959–1976.

Ogoshi, T., Chujo, Y., 2003. Synthesis of organic–inorganic polymer hybrids by means of host–guest interaction utilizing cyclodextrin. Macromolecules 36 (3), 654–660.

Ohira, A., Sakata, M., Taniguchi, I., Hirayama, C., Kunitake, M., 2003. Comparison of nanotube structures constructed from α-, β-, and γ-cyclodextrins by potential-controlled adsorption. J. Am. Chem. Soc. 125, 5057–5065.

Okumura, Y., Ito, K., Hayakawa, R., Nishi, T., 2000. Self-assembling dendric supramolecule of molecular nanotubes and starpolymers. Langmuir 16, 10278–10280.

Olaf, H., Muller-Goymann, C.C., 1993. Properties and structure of aqueous solutions of hydroxypropyl-beta-cyclodextrin. Starch 45, 183–187.

Parazak, D.P., Khan, A.R., DSouza, V.T., Stine, K.J., 1996. Comparison of host–guest Langmuir–Blodgett multilayer formation by two different amphiphilic cyclodextrins. Langmuir 12 (16), 4046–4049.

Péroche, S., Degobert, G., Putaux, J.L., Blanchin, M.G., Fessi, H., Parrot-Lopez, H., 2005. Synthesis and characterisation of novel nanospheres made from amphiphilic perfluoroalkylthio-beta-cyclodextrins. Eur. J. Pharmaceut. Biopharmaceut. 60, 123–131.

Pistolis, G., Malliaris, A., 1996. Nanotube formation between cyclodextrins and 1,6-diphenyl-1,3,5-hexatriene. J. Physical Chem. 100 (38), 15562–15568.

Pistolis, G., Malliaris, A., 1998. Size effect of alpha,omega-diphenylpolyenes on the formation of nanotubes with gamma-cyclodextrin. J. Physical Chem. B 102 (7), 1095–1101.

Polarz, S., Smarsly, B., Bronstein, L., Antonietti, M., 2001. From cyclodextrin assemblies to porous materials by silica templating. Angew. Chem. Int. Ed. 40, 4417–4421.

Quaranta, A., Zhang, Y.M., Filippone, S., Yang, J., Sinay, P., Rassat, A., Edge, R., Navaratnam, S., McGarvey, D.J., Land, E.J., Brettreich, M., Hirsch, A., Bensasson, R.V., 2006. Photophysical studies of six amphiphilic 2:1 cyclodextrin:[60]fullerene derivatives. Chem. Phys. 325 (2), 397–403.

Ravoo, B.J., Darcy, R., 2000. Cyclodextrin bilayer vesicles. Angew. Chem. 112 (23), 4494–4496.

Ravoo, B.J., Darcy, R., Mazzaglia, A., Nolan, D., Gaffney, K., 2001. Supramolecular tapes formed by a catanionic cyclodextrin in water. Chem. Commun. 9, 827–828.

Rekharsky, M.V., Inoue, Y., 1998. Complexation thermodynamics of cyclodextrins. Chem. Rev. 98, 1875–1917.

Roy, D., Mondal, S.K., Sahu, K., Ghosh, S., Sen, P., Bhattacharyya, K., 2005. Temperature dependence of anisotropy decay and solvation dynamics of coumarin 153 in gamma-cyclodextrin aggregates. J. Physical Chem. A 109 (33), 7359–7364.

Saenger, W., Jacob, J., Gessler, K., Steiner, T., Hoffmann, D., Sanbe, H., Koizumi, K., Smith, S.M., Takaha, T., 1998. Structures of the common cyclodextrins and their larger analogues-beyond the doughnut. Chem. Rev. 98, 1787–1802.

Samitsu, S., Shimomura, T., Ito, K., Hara, M., 2004. Immobilization of molecular tubes on self-assembled monolayers of beta-cyclodextrin and dodecanethiol inclusion complexes. Appl. Phys. Lett. 85 (17), 3875–3877.

Sau, S., Solanki, B., Orprecio, R., Van Stam, J., Evans, C.H., 2004. Higher-order cyclodextrin complexes: the naphthalene system. J. Inclusion Phenomena Macrocyclic Chem. 48 (3–4), 173–180.

Selva, A., Redenti, E., Ventura, P., Zanol, M., Casetta, B., 1998. Study of beta-cyclodextrin-ketoconazole-tartaric acid multicomponent non-covalent association by positive and negative ionspray mass spectrometry. J. Mass Spectrom. 33 (8), 729–734.

Shen, X.H., Belletete, M., Durocher, G., 1997. Studies of the inclusion complexation between a 3H-indole and beta-cyclodextrin in the presence of urea, sodium dodecyl sulfate, and 1-propanol. Langmuir 13 (22), 5830–5836.

Shen, X.H., Belletete, M., Durocher, G., 1998. Spectral and photophysical studies of the 1:3 (guest/host) rotaxane-like inclusion complex formed by a 3H-indole and beta-cyclodextrin. J. Physical Chem. B 102 (11), 1877–1883.

Shen, X.H., Belletete, M., Durocher, G., 1999. Interactions between a surface-active cationic 3H-indole molecular probe and beta-cyclodextrin. Design of a novel type of rotaxane. Chem. Phys. Lett. 301 (1–2), 193–199.

Shigekawa, H., Miyake, K., Sumaoka, J., Harada, A., Komiyama, M., 2000. The molecular abacus: STM manipulation of cyclodextrin necklace. J. Am. Chem. Soc. 122 (22), 5411–5412.

Shinohara, K.I., Suzuki, T., Kitami, T., Yamaguchi, S., 2006. Simultaneous imaging of the structure and fluorescence of a supramolecular nanostructure formed by the coupling of pi-conjugated polymer chains in the intermolecular interaction. J. Polymer Sci. Part A: Polymer Chem. 44 (2), 801–809.

Szejtli, J., 1998. Introduction and general overview of cyclodextrin chemistry. Chem. Rev. 98 (5), 1743–1753.

Szente, L., Szejtli, J., Kis, G.L., 1998. Spontaneous opalescence of aqueous gama-cyclodextrin solutions: complex formation or self-aggregation? J. Pharmaceut. Sci. 87 (6), 778–781.

Tchoreloff, P.C., Boissonnade, M.M., Coleman, A.W., Baszkin, A., 1995. Amphiphilic monolayers of insoluble cyclodextrins at the water air interface – surface pressure and surface-potential studies. Langmuir 11 (1), 191–196.

Udachin, K.A., Wilson, L.D., Ripmeester, J.A., 2000. Solid polyrotaxanes of polyethylene glycol and cyclodextrins: the single crystal X-ray structure of PEG-beta-cyclodextrin. J. Am. Chem. Soc. 122 (49), 12375–12376.

van den Boogaard, M., Bonnet, G., van't Hof, P., Wang, Y., Brochon, C., van Hutten, P., Lapp, A., Hadziioannou, G., 2004. Synthesis of insulated single-

chain semiconducting polymers based on polythiophene, polyfluorene, and beta-cyclodextrin. Chem. Mater. 16 (23), 4383–4385.

Wang, J., Jiang, M., 2006. Polymeric self-assembly into micelles and hollow spheres with multiscale cavities driven by inclusion complexation. J. Am. Chem. Soc. 128 (11), 3703–3708.

Wen, X.H., Guo, M., Liu, Z.Y., Tan, F., 2004. Nanotube formation in solution between beta-cyclodextrin and cinchonine. Chem. Lett. 33 (7), 894–895.

Wenz, G., 1994. Cyclodetrins as building for supermolecular structures and functional units. Angew. Chem. Int. Ed. 33, 803–822.

Wenz, G., Han, B.H., Muller, A., 2006. Cyclodextrin rotaxanes and polyrotaxanes. Chem. Rev. 106 (3), 782–817.

Wu, A.H., Ph.D. Thesis, Peking University, Beijing, 2006.

Wu, A.H., Shen, X.H., Gao, H.C., 2006a. Cyclodextrin nanotube induced by 4,4′-bis(2-benzoxazolyl) stilbene. Int. J. Nanosci. 5 (2–3), 213–218.

Wu, A.H., Shen, X.H., He, Y.K., 2006b. Investigation on γ-cyclodextrin nanotube induced by *N*,*N*′-diphenylbenzidine molecule. J. Colloid Interface Sci. 297, 525–533.

Wu, A.H., Shen, X.H., He, Y.K., 2006c. Micrometer-sized rodlike structure formed by the secondary assembly of cyclodextrin nanotube. J. Colloid Interface Sci. 302 (1), 87–94.

Liu, Y., You, C.C., Zhang, H.Y., Kang, S.Z., Zhu, C.F., Wang, C., 2001. Bis(molecular tube)s: supramolecular assembly of complexes of organoselenium-bridged beta-cyclodextrins with platinum(IV). Nano Lett. 1 (11), 613–616.

Yang, L., Takisawa, N., Kaikawa, T., Shirahama, K., 1997. Interaction of photosurfactants 2-[4-(4-alkylphenylazo)phenoxy]ethyltrimethyl-ammonium bromides with γ-cyclodextrin and thermodynamics of complexation of photosurfactants with cyclodextrins. Colloid Polymer Sci. 275 (5), 486–492.

Yazdanparast, R., Esmaeili, M.A., Khodarahmi, R., 2006. Protein refolding assisted by molecular tube based alpha-cyclodextrin as an artificial chaperone. Biochemistry (Moscow) 71 (12), 1298–1306.

Yoshida, K., Shimomura, T., Ito, K., Hayakawa, R., 1999. Inclusion complex formation of cyclodextrin and polyaniline. Langmuir 15 (4), 910–913.

Zhang, C.F., Shen, X.H., Gao, H., 2002. Studies on the nanotubes formed by 2-phenyl-5-(4-diphenylyl)1,3,4-oxadiazole and cyclodextrins. Chem. Phys. Lett. 363, 515–522.

Zhang, C.F., Shen, X.H., Gao, H., 2003. Studies on the formation of cyclodextrin nanotube by fluorescence and anisotropy measurements. Spectrosc. Spectral Anal. 23 (2), 217–220.